

KEY ISSUES REVIEW

Two-photon interference: the Hong–Ou–Mandel effect

To cite this article: Frédéric Bouchard *et al* 2021 *Rep. Prog. Phys.* **84** 012402

View the [article online](#) for updates and enhancements.

You may also like


- [Signatures of many-particle interference](#)
Mattia Walschaers
- [Theory of scanning tunneling spectroscopy: from Kondo impurities to heavy fermion materials](#)
Dirk K Morr
- [Many-body interference in bosonic dynamics](#)
Gabriel Dufour, Tobias Br  nner, Alberto Rodriguez et al.

www.hidenanalytical.com
info@hiden.co.uk

HIDEN ANALYTICAL


Instruments for Advanced Science

Mass spectrometers for vacuum, gas, plasma and surface science



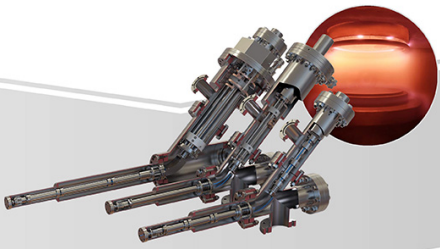
Residual Gas Analysis

Perform RGA at UHV/XHV. Our RGA configurations include systems for UHV science applications including temperature-programmed desorption and electron/photon stimulated desorption.




Thin Film Surface Analysis


Conduct both static and dynamic SIMS analysis with a choice of primary ions for full chemical composition and depth profiling. Our SIMS solutions include complete workstations and bolt-on modules.



Plasma Characterisation

Fully characterise a range of plasmas: RF, DC, ECR and pulsed plasmas, including neutrals and neutral radicals. Extend your analyses to atmospheric pressure processes using the HPR-60, with time-resolved mass/energy analysis.

 www.HidenAnalytical.com

 info@hiden.co.uk

Key Issues Review

Two-photon interference: the Hong–Ou–Mandel effect

Frédéric Bouchard^{1,5}, Alicia Sit¹, Yingwen Zhang², Robert Fickler^{1,6} ,
Filippo M Miatto³, Yuan Yao³, Fabio Sciarrino⁴  and Ebrahim Karimi^{1,2,*} 

¹ Department of Physics, University of Ottawa, Advanced Research Complex, 25 Templeton Street, Ottawa ON K1N 6N5, Canada

² National Research Council of Canada, 100 Sussex Drive, Ottawa, Ontario K1A 0R6, Canada

³ Télécom Paris, LTCI, Institut Polytechnique de Paris, 19 Place Marguerite Peray, 91120 Palaiseau, France

⁴ Dipartimento di Fisica, Sapienza Università di Roma, Piazzale Aldo Moro 5, I-00185 Roma, Italy

E-mail: ekarimi@uottawa.ca

Received 27 June 2020, revised 2 November 2020

Accepted for publication 24 November 2020

Published 24 December 2020



Abstract

Nearly 30 years ago, two-photon interference was observed, marking the beginning of a new quantum era. Indeed, two-photon interference has no classical analogue, giving it a distinct advantage for a range of applications. The peculiarities of quantum physics may now be used to our advantage to outperform classical computations, securely communicate information, simulate highly complex physical systems and increase the sensitivity of precise measurements. This separation from classical to quantum physics has motivated physicists to study two-particle interference for both fermionic and bosonic quantum objects. So far, two-particle interference has been observed with massive particles, among others, such as electrons and atoms, in addition to plasmons, demonstrating the extent of this effect to larger and more complex quantum systems. A wide array of novel applications to this quantum effect is to be expected in the future. This review will thus cover the progress and applications of two-photon (two-particle) interference over the last three decades.

Keywords: quantum optics, quantum computation, quantum cryptography

(Some figures may appear in colour only in the online journal)

1. Introduction

At the inception of quantum mechanics, a series of seminal experiments were performed showing the superposition principle. For instance, the double-slit experiment, with photons or electrons, demonstrates the interference of a single particle with itself, revealing the ‘blurring’ of the quantum

wavefunction prior to measurement. Such sort of experiments open up fundamental and philosophical questions regarding the non-local (and contextual) nature of quantum mechanics. Although, for the case of particles, superposition and interference remain counterintuitive and surprising, when applied to classical waves, they become instinctive and common [1]. Thus, quantum phenomena arising from the wave-particle duality does not encapsulate the whole essence of quantum weirdness. In the search for the ‘most’ quantum phenomenon, three groups—Hong–Ou–Mandel (HOM), Fearn–Loudon, and Rarity–Tapster—independently investigated the interference of ‘quantum paths’, all within a couple of years during the late 1980s. As to the precise ordering of who ‘discovered’—or

* Author to whom any correspondence should be addressed.

⁵ Current address: National Research Council of Canada, 100 Sussex Drive, Ottawa, Ontario K1A 0R6, Canada

⁶ Current address: Photonics Laboratory, Physics Unit, Tampere University, Tampere, FI-33720, Finland

Corresponding editor: Professor Masud Mansuripur.

rather more appropriately ‘clarified’—this new effect first is perhaps only known to a few and the original authors themselves; however, in the interest of being unbiased, we recount here only the story of *two-photon interference* as historically reported by the literature.

Beginning in early 1987, several theoretical papers were published in quick succession which formulated the action of the humble beam splitter (BS) in terms of quantum mechanics. To start, Prasad, Scully, and Martienssen derived the unitary transformation that couples the input mode set to the outgoing transmitted and reflected mode set [2]. A brief comment is made on the consequence of having a non-zero number state in each input mode, stating that a highly correlated superposition of states is created, given by the different ways the total number of input photons can be distributed between the two output modes. Of interest is that a general formulation for the transformed output state is given (in which two-photon interference is embedded, but not mentioned), with a footnote pertaining to private communication with Loudon, whose own work on this subject was forthcoming as we will see.

Published two months later in the same journal, we find a paper by Ou, Hong, and Mandel outlining how to express the output of a BS using the diagonal coherent state representation [3]; in particular, they give the explicit example of what happens when two photons, one horizontally and one vertically polarized, are incident from different input ports. Indeed, they note that, for a balanced BS, the simultaneous detections at the two output ports behaves like the singlet state for two orthogonally polarized photons, i.e. a Bell state measurement, as we know it today. In tandem with their theoretical work, we come to the (seminal) experimental work by Hong, Ou, and Mandel demonstrating that this interference of two identical photons at a BS, shown as the hallmark ‘dip’ in coincidence detections at the output, can be used to measure very short time intervals [4]. Barely a month later, the work of Fearn and Loudon formulating the action of a lossless BS is published, presumably that which was hinted at by Prasad, Scully, and Martienssen, looking more rigorously into the physics through quantization in terms of both the input and output mode contributions [5]. Finally, our last set of players who investigated this two-photon interference effect around the same time as Hong-Ou-Mandel and Fearn–Loudon are Rarity and Tapster. A conference paper of theirs appears in a workshop book, outlining the nonclassical effect in parametric downconversion [6], and later published as a separate paper [7]. Much like Hong-Ou-Mandel, Rarity and Tapster experimentally demonstrate two-photon interference from parametric down conversion for the use of subpicosecond measurements. Another experiment of note appearing at the beginning of this time period is, for example, the work by Abram, Raj, Oudar and Dolique in 1986 which explored the second-order coherence of parametric down conversion [8]. Curiously, a two-photon interferometer was demonstrated in 1986 by Alley and Shih, as noted in [9]; however, their results were published in 1988. They performed correlation measurements on two identically polarized photons that were superposed on a BS, observing maximum and minimum coincidences for measurements with parallel and perpendicularly-aligned polarizers, respectively.

No matter the historical details, two-photon interference—popularly termed now as the Hong-Ou-Mandel (HOM) effect—has been referred to as ‘the heart of quantum mechanics’ for being exquisitely quantum in nature, with absolutely no analogue in classical physics. It is precisely this separation from classical to quantum physics that gives two-photon interference a distinct advantage to outperform classical computations, securely communicate information, simulate highly complex physical systems and increase the sensitivity of precise measurements. It has also motivated physicists to study more generally two-particle interference for fermionic and bosonic quantum objects, with successful experiments using massive particles, among others, such as electrons and atoms, in addition to plasmons, demonstrating the extent of this effect to larger and more complex quantum systems. A wide array of novel applications to this quantum effect is to be expected in the future.

This review attempts to aggregate the most prevalent uses of two-photon interference over the past three decades into one coherent text. To be consistent with the present-day literature, we will simply refer to two-photon (particle) interference as the HOM effect hereafter, or simply HOM for brevity. We begin with the fundamental theory behind the HOM effect in an intuitive manner, along with the experimental considerations. After this, the majority of the review details the many uses of HOM in the optical domain: precise measurements (as per the intention of the original experimental paper), quantum state analysis/engineering, quantum communication/computation, and a generalization to multipartite and multimode systems. Of course, the HOM effect is not limited to photons, and thus we close the review with implementations in non-photon systems, such as plasmons, phonons, atoms and electrons.

1.1. Action of the beam splitter

The action of the beam splitter (BS) is at the heart of the two-photon interference effect, providing the mixing between the two input modes. Formally, it can be represented by a unitary transformation, thus conserving energy and preserving orthogonality between input states. Although simple, the BS is an essential building block of any linear optical quantum information processing system. As a starting point for the theory of the HOM effect, we establish the theoretical framework describing the operational action of the BS.

A BS is an optical device with two input ports, labelled a and b , and two output ports, labelled c and d , see figure 1. A beam incident on a BS at the input port a , or similarly for b , is split between output ports c and d in proportions depending on complex parameters r and t , known as the reflectance and transmittance of the BS, here taken to be lossless. From this point forward, we will consider the prominent case of the balanced BS where $|r| = |t| = 1/\sqrt{2}$, also known as the 50:50 BS. Classically, the electric fields in output modes c and d are given in terms of the electric fields in the input modes according to $E_c = (E_a + E_b)/\sqrt{2}$ and $E_d = (E_a - E_b)/\sqrt{2}$, where we have chosen a specific phase relation between the reflected and transmitted beams. In particular, this phase relation depends on technical design of the BS, e.g. number of

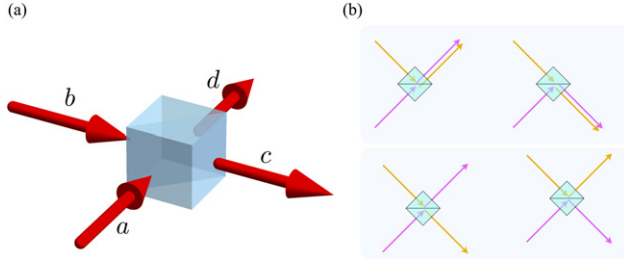


Figure 1. Action of a beam splitter. (a) Beam splitter with input ports labelled a and b , and output ports labelled c and d . Arrows indicate the field propagation directions. (b) The four ways the two photons can exit from the beam splitter—through the same port (top row) or different ports (bottom row).

dielectric layers and the coating design [10]. Nevertheless, the physical aspects of the BS discussed hereafter are not affected by this phase relation, as long as energy conservation and unitarity are fulfilled.

We are now ready to move to the quantum description of the BS according to the *second quantization* formalism. This is done by employing a set of bosonic annihilation and creation operators (\hat{a}_i and \hat{a}_i^\dagger , respectively) to represent electromagnetic fields in mode i . The annihilation and creation operators must satisfy the standard bosonic commutation relation, i.e. $[\hat{a}_i, \hat{a}_j^\dagger] = \delta_{ij}$, where δ_{ij} is the Kronecker delta symbol. Explicitly, the effect of the creation operator acting on the vacuum is given by,

$$(\hat{a}_i^\dagger)^n |0\rangle = \sqrt{n!} |n\rangle_i, \quad (1)$$

where $|0\rangle$ is the vacuum state and $|n\rangle_i$ is an n -photon Fock state in mode i . For the input and output modes shown in figure 1, we use the notation \hat{a} , \hat{b} , \hat{c} and \hat{d} to represent annihilation operators in modes a , b , c and d , respectively. Hence, the operation of a 50:50 BS is given in terms of field operators by,

$$\begin{cases} \hat{a} = \frac{1}{\sqrt{2}} (\hat{c} + \hat{d}) \\ \hat{b} = \frac{1}{\sqrt{2}} (\hat{c} - \hat{d}) \end{cases}, \quad (2)$$

where we have inverted the transformation by representing the input annihilation operators in terms of the output annihilation operators. We have now laid out the theoretical framework necessary to describe the two-photon interference effect.

1.2. Two-photon interference

The two-photon interference effect is traditionally introduced as follows: assume two photons are incident at each input port of a 50:50 BS. Let us additionally consider that the two photons may be distinguished due to an additional degree of freedom, for example polarization, timing, frequency or spatial modes. Using the notation introduced above, we consider the initial state as $|\psi_{\text{in}}\rangle = |1\rangle_{a,H} |1\rangle_{b,V} = |H\rangle_a |V\rangle_b = \hat{a}_H^\dagger \hat{b}_V^\dagger |0\rangle$, where \hat{a}_H^\dagger and \hat{b}_V^\dagger are the creation operators corresponding to the modes of *horizontally* polarized light in input port a , $|H\rangle_a$, and *vertically* polarized light in input port b , $|V\rangle_b$, respectively. Using the BS transformation relations from

equation (2), the output state is given by,

$$\begin{aligned} \hat{a}_H^\dagger \hat{b}_V^\dagger |0\rangle &\xrightarrow{\text{BS}} \frac{1}{2} (\hat{c}_H^\dagger + \hat{d}_H^\dagger) (\hat{c}_V^\dagger - \hat{d}_V^\dagger) |0\rangle \\ &= \frac{1}{2} (\hat{c}_H^\dagger \hat{c}_V^\dagger - \hat{c}_H^\dagger \hat{d}_V^\dagger + \hat{c}_V^\dagger \hat{d}_H^\dagger - \hat{d}_H^\dagger \hat{d}_V^\dagger) |0\rangle. \end{aligned} \quad (3)$$

From the output state, we can infer four distinct possibilities for the two photons: the two photons exit the BS together through the same output port, corresponding to the first and last terms above, i.e. $\hat{c}_H^\dagger \hat{c}_V^\dagger$ and $\hat{d}_H^\dagger \hat{d}_V^\dagger$, or the photons exit the BS separately through different output ports, corresponding to the second and third terms above, i.e. $\hat{c}_H^\dagger \hat{d}_V^\dagger$ and $\hat{c}_V^\dagger \hat{d}_H^\dagger$. With no surprises, we obtain all the classically expected outcomes.

The two-photon interference now occurs when considering indistinguishable photons. Starting from equation (3), let the two input photons have the same polarization state, such that they are identical. For simplicity, we can then remove the polarization subscripts such that the output state now reads,

$$\begin{aligned} \hat{a}^\dagger \hat{b}^\dagger |0\rangle &\xrightarrow{\text{BS}} \frac{1}{2} (\hat{c}^\dagger \hat{c}^\dagger - \hat{c}^\dagger \hat{d}^\dagger + \hat{c}^\dagger \hat{d}^\dagger - \hat{d}^\dagger \hat{d}^\dagger) |0\rangle \quad (4) \\ &= \frac{1}{2} ((\hat{c}^\dagger)^2 - (\hat{d}^\dagger)^2) |0\rangle \\ &= \frac{1}{\sqrt{2}} (|2\rangle_c - |2\rangle_d). \end{aligned} \quad (4)$$

Astonishingly, we find a new type of interference effect, physically distinct from the interference of a single photon or classical fields, where it is the overall two-photon states that interfere. In this case, we observe destructive interference of the two-photon states corresponding to photons exiting opposite output ports, and constructive interference of the two-photon states corresponding to photons exiting through the same output ports. If a coincidence-type measurement were to be performed, where a single photon detector is placed in each output port, zero coincidence events would be observed. Nevertheless, destructive and constructive interference can be adjusted by tailoring the symmetry of the overall input two-photon state, as will be discussed in the following section, noting again that the relative phase is inconsequential. Note, in the case of fermionic particles, say electrons, the creation operators will anti-commute, implying that $\hat{c}^\dagger \hat{d}^\dagger = -\hat{d}^\dagger \hat{c}^\dagger$. Therefore, $|1\rangle_a |1\rangle_b \xrightarrow{\text{BS}} |1\rangle_c |1\rangle_d$ and the fermions will exit through different output ports. This will be discussed in more details in section 8.

If classical, independent light sources are incident at the input ports, there will be a 50% chance of observing coincidence events due to random correlations. This gives the classical limit of 0.5 [11]. Nonetheless, there have been several studies that explore using classical light sources, such as weak coherent pulses or thermal light, as an alternative resource for implementing two-photon interference [12–17] for the use in various quantum technologies such as quantum key distribution (QKD) [18].

It may seem that the HOM effect requires the two photons entering the BS to be indistinguishable. However, some works have suggested that this indistinguishability for photons generated via SPDC is not strictly necessary at the BS, but at the detectors [19, 20]. Here, two distinguishable photons, with orthogonal polarizations and generated in a type-II crystal, enter the BS with a time difference greater than the coherence time of the photons. The time difference was then compensated after the BS in such a way that the difference in arrival time between the two photons at the detectors, in the cases where both photons are reflected and both are transmitted, are indistinguishable. The photons' polarizations were also made indistinguishable by the placement of two polarizers before the detectors. As both the arrival time difference and the polarization between the photons are made indistinguishable, the HOM dip/peak can once again be observed. Interestingly, the two distinguishable photons are now also polarization-entangled. Recently, HOM interference between temporally separated continuous-wave coherent photons by using a temporal post-selection method with a time delay of up to one day has been demonstrated [21].

1.3. Entangled states

In addition to being one of the most peculiar phenomenon in quantum optics, two-photon interference is one of the primary tools used in quantum information processing. At the heart of quantum information is the notion of quantum entanglement [22]—the fundamental resource in quantum communication [23], quantum metrology [24], and quantum computing [25]. Quantum entanglement inherently deals with the interference of two-photon states, thus hinting to the fact that the HOM effect might play an important role in the engineering and analysis of entangled states. Although the extension of the HOM effect to multi-photon (more than two photons) will be discussed in section 7, we will now concentrate on the case of two photons.

Two-photon bidimensional entanglement is conveniently built upon the basis of maximally entangled states, also known as the *Bell states*. Using once again the example of polarization, the Bell states are given by:

$$|\Psi^\pm\rangle_{ab} = \frac{1}{\sqrt{2}} (|H\rangle_a |V\rangle_b \pm |V\rangle_a |H\rangle_b) \quad (5)$$

$$|\Phi^\pm\rangle_{ab} = \frac{1}{\sqrt{2}} (|H\rangle_a |H\rangle_b \pm |V\rangle_a |V\rangle_b), \quad (6)$$

where $|H\rangle$ and $|V\rangle$ represent a one-photon state in the mode of horizontal and vertical linear polarization, respectively. As a first step, let us directly apply a similar calculation, as previously shown, to determine the output state at a 50:50 BS when the Bell states are considered as the input states. After some calculations, we obtain,

$$|\Psi^+\rangle_{ab} \xrightarrow{\text{BS}} \frac{1}{\sqrt{2}} (\hat{c}_H^\dagger \hat{c}_V^\dagger - \hat{d}_H^\dagger \hat{d}_V^\dagger) |0\rangle,$$

$$|\Psi^-\rangle_{ab} \xrightarrow{\text{BS}} \frac{-1}{\sqrt{2}} (\hat{c}_H^\dagger \hat{d}_V^\dagger - \hat{c}_V^\dagger \hat{d}_H^\dagger) |0\rangle,$$

$$|\Phi^\pm\rangle_{ab} \xrightarrow{\text{BS}} \frac{1}{2\sqrt{2}} \left((\hat{c}_H^\dagger)^2 \pm (\hat{c}_V^\dagger)^2 - (\hat{d}_H^\dagger)^2 \mp (\hat{d}_V^\dagger)^2 \right) |0\rangle. \quad (7)$$

After examination of the Bell states after passing through the BS, we notice a few interesting features. For the $|\Psi^+\rangle$ state, we may notice that the output photons always exit the BS together through the same output ports, just as in the case of indistinguishable photons discussed previously, i.e. $|1\rangle_a |1\rangle_b$. This type of behaviour, known as ‘*bunching*’, is also observed for input states $|\Phi^\pm\rangle$. However, for the case of $|\Psi^-\rangle$, we observe the output photons always exiting the BS in opposite output ports, also known as ‘*anti-bunching*’. Interestingly, bunching and anti-bunching are typical *bosonic* and *fermionic* behaviours, respectively. Indeed, those behaviours can be understood from the symmetry of the Bell states [26]. By definition, a system of bosons is symmetric under the exchange of any pair, whereas a system of fermions is anti-symmetric under the exchange of any pair. Hence, due to their bosonic nature, photon pairs must be in an overall symmetric state, which is clearly the case for $|\Psi^+\rangle$ and $|\Phi^\pm\rangle$. However, although the $|\Psi^-\rangle$ is said to be the ‘anti-symmetric state’ and exhibits anti-bunching, its overall state, including polarization together with path, *must* be symmetric. Indeed, both the polarization and the path degree of freedom of the photon pair are individually anti-symmetric, leaving the overall state symmetric. Hence, the ability to discriminate the $|\Psi^-\rangle$ Bell state, by taking advantage of its fermionic behaviour, is central to the concept of *Bell state analysis*, as will be discussed in a forthcoming section.

1.4. Two-photon interference with qudits

Here, we extend the HOM effect to higher dimensions. We use the notation $|n\rangle_i$ to describe an n photon number state of mode i , see equation (1). Recall that a mode can be defined by polarization, frequency and spatial degrees of freedom. To define a d -dimensional basis, we pick d modes, $\{‘0’, ‘1’, \dots, ‘d-1’\}$, and we populate them with one photon in total. We are therefore working within the 1-photon multiplet of the total photon number operator $\hat{n} = \sum_i \hat{a}_i^\dagger \hat{a}_i$.

Let us consider two qudit photon states ($|\phi\rangle = \sum_{i=0}^{d-1} \alpha_i |1\rangle_i$, and $|\psi\rangle = \sum_{j=0}^{d-1} \beta_j |1\rangle_j$) incident on a 50:50 BS, where the notation implies that the omitted modes are all in vacuum. If we input these two states at different input ports, we obtain:

$$|\phi\rangle |\psi\rangle = \sum_{i=0}^{d-1} \alpha_i \beta_j \left(\frac{|2\rangle_i |0\rangle_j - |0\rangle_i |2\rangle_j}{\sqrt{2}} \right) + \sum_{i \neq j=0}^{d-1} \left(\frac{\alpha_i \beta_j - \alpha_j \beta_i}{2} \right) |1\rangle_i |1\rangle_j. \quad (8)$$

The coincidence probability is given by the last term in equation (8), i.e.

$$\sum_{i \neq j=0}^{d-1} \frac{1}{4} (\alpha_i \beta_j - \alpha_j \beta_i) (\alpha_i \beta_j - \alpha_j \beta_i)^* = \frac{1 - |\langle \phi | \psi \rangle|^2}{2}, \quad (9)$$

and the two-photon probability is then $(1 + |\langle \phi | \psi \rangle|^2) / 2$. We note that when $|\phi\rangle$ and $|\psi\rangle$ are identical there will be no coincidences and the last term in equation (8) will vanish. While for completely distinguishable states, i.e. $\langle \phi | \psi \rangle = 0$, the two photons will bunch half of the time. Thus, HOM can be adopted as a powerful tool to directly measure the overlap between two single photon wavepackets. Following these ideas, HOM has been also used to demonstrate the quantum nature of orthogonal transverse spatial modes, i.e. their azimuthal [27] as well as their radial mode structure [28]. In addition, HOM has not only been observed as bunching into the same paths but in various different photonic degrees of freedom, polarization [29], transverse spatial modes in free space [30, 31] as well as waveguides [32], and also frequency modes [33, 34].

2. Precision measurements

In the original paper by Hong, Ou and Mandel [4] (as well as Rarity and Tapster [6]), the quantum optical formalism of the two-photon interference is presented and the famous HOM dip is experimentally observed. As will be discussed in the upcoming sections, the two-photon interference is fundamental to a plethora of quantum information tasks. Nevertheless, Hong, Ou and Mandel present the HOM dip and discuss its applications in terms of precise timing measurement. In particular, they draw the link between their scheme and the well known techniques used to measure short pulses using nonlinear materials, e.g. intensity auto-correlation. Subpicosecond time intervals can now be measured for photon pairs from parametric down-conversion going far beyond the previous timing resolution of standard photodetectors, i.e. larger than 100 ps. Since then, several experiments have investigated the use of the HOM effect to perform precise timing measurements.

2.1. Precise timing measurement

In recent years, there has been a renewed interest in using the HOM effect to measure minute time variations. Motivated by the body of work on structured light that has emerged in the last few decades [35], an interest in the propagation of structured beams in free-space led to a series of experiments measuring time shifts due to the modal structure of the propagating beams [36–39]. In some of these experiments, a shift in the HOM dip was used to evaluate a temporal shift due to the spatial structure of the beam [35].

A general setup to perform precise timing measurements using HOM is shown in figure 2(a). As an aside, it is possible to obtain HOM using different configurations of interferometers, for example, using a Mach–Zehnder interferometer [40, 41] or a non-local Franson interferometer [42]. In the first of these experiments [36], the group velocity of single photons with the profile of a Bessel beam and a focused Gaussian beam is compared to that of a collimated Gaussian beam. In this experiment, entangled photon pairs are generated through spontaneous parametric down-conversion (SPDC), and the signal and idler photons are separated using a knife-edge mirror. It is the signal photon that experiences the time shift, due to a variation in its group velocity. In [36], the variation in group velocity

is induced by structuring the transverse profile of the signal photon. This is achieved by sending the signal photon onto a spatial light modulator (SLM) which can be programmed to act as a diffractive optical element implementing axicons or lenses to modulate the photons into a Bessel beam or a focused Gaussian beam. The signal photon is then allowed to propagate in free space before arriving at a second SLM which reverses the structure of the photon introduced by the first SLM. The signal photon is then made incident onto one of the input ports of a 50:50 BS with the idler photon incident in the other input port. By varying the path length of one of the photons and recording coincidence counts at the output port of the BS, the HOM dip is measured where the minimum of the dip sets a time reference. As a next step, the signal photon's group velocity can be varied using the SLMs, resulting in a different time shift which can be observed by a shifted HOM dip. The shift of the HOM dip is then related to a direct time shift in the arm of the signal photon. In another experiment, variations in the time of flight is also investigated using a similar experimental setup [38]. In this case, time shifts arise by varying the optical orbital angular momentum (OAM) value of the signal photon. The addition of OAM in the phase of the beam is compared to a beam with the same intensity profile at the SLM, but no net OAM. Once again, the HOM effect is used as a highly precise timing measurement tool.

In the works mentioned above, a noncommon-path HOM interferometer is employed to measure time shifts with resolutions on the order of a few femto-seconds (micrometers), where the time shifts are obtained by assessing the shift of the HOM dip. Thus, one might expect the limit on time resolutions of this apparatus to be given by the width of the HOM dip, or equivalently the coherence time of the photons. According to this argument, larger time resolutions can be achieved by employing ultra-broadband single photon sources. However, it has recently been shown that, by considering the limits dictated by statistical estimation theory, it is possible to push the time resolution of an HOM interferometer to sub-femtosecond resolutions [43]. At the heart of estimation theory, is the Cramér–Rao bound which poses the ultimate limit on the precision of the estimation of a parameter, in this case the time shift. In the work of [43], a standard HOM interferometer, similar to the one shown in figure 2, is used to measure a time shift. In particular, the Cramér–Rao bound is saturated using the maximum-likelihood estimator, and the Fisher information—which depends on the coherence time of the photons, the visibility of the HOM dip, and losses—is maximized. By doing so, an average accuracy and average precision of 6 attoseconds and 16 attoseconds were achieved, respectively. Moreover, it is also possible to maximize the Fisher information by custom-tailoring the state of the probe photons using frequency entanglement [44], and by using detector timing and number resolving abilities [45].

2.2. Quantum optical coherence tomography

Another particularity of the two-photon interference is its inherent dispersion cancelation, which does not occur in the case of the one-photon interference, or the interference of

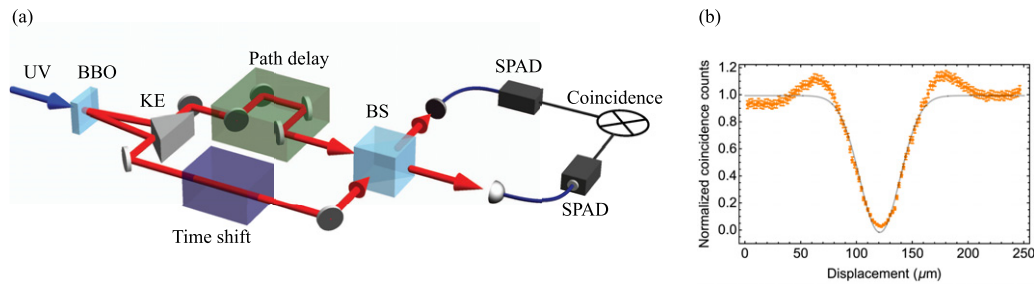


Figure 2. Simplified experimental setup to observe the Hong–Ou–Mandel dip. (a) We present an experimental setup similar to that presented by Hong, Ou and Mandel. An ultraviolet (UV) laser pumps a nonlinear crystal, e.g. KDP, BBO or ppKTP. Pairs of photons are generated with anti-correlated linear momentum and separated using a knife-edge (KE) mirror. The photons are brought back together at a 50:50 BS, where a variable path delay is scanned to control the arrival time of one of the photons. The photons exiting the output ports of the BS are detected using single-photon avalanche diode (SPAD) detectors and coincidence counts are recorded. (b) Example of experimental results showing the two-photon interference dip, dropping to zero when the two photons enter the BS simultaneously. Solid line indicated expected theoretical coincidence counts, and dots indicate experimental measurements. The peak in counts on either side of the dip is caused by the use of a rectangular bandpass filter in experiment, as compared to a Gaussian filter in theory. Figure legends: UV, ultraviolet beam; BBO, Beta barium borate nonlinear crystal; KE, knife edge; BS, 50:50 beam splitter; SPAD, single photon avalanche diode.

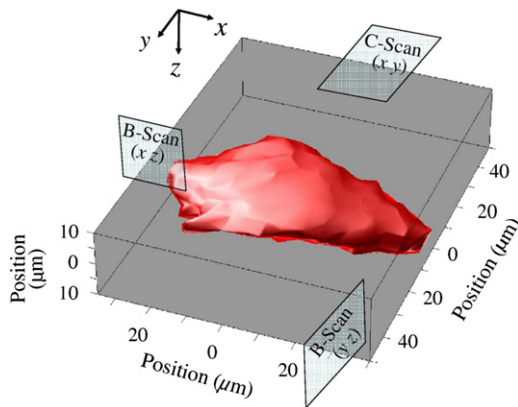


Figure 3. Example of quantum optical coherence tomography. 3-dimensional image of onion-skin tissue coated with gold nano-particles taken with QOCT. Reprinted from [53], Copyright (2009), with permission from Elsevier.

classical light. In particular, it is the even-order effects of dispersion, such as group-velocity dispersion, that are cancelled [46]. Thus, the two-photon interference effect holds great potential for applications where dispersion can seriously limit optical applications. A great example of such an application is the medical imaging technique known as optical coherence tomography (OCT), where a low-coherence light source is used in an interferometric setup to reconstruct the 2-dimensional or 3-dimensional profile of tissues [47]. In theory, the resolution of OCT is limited by the coherence length of the light source; however, in practice, it is the material dispersion that limits the resolution.

In order to overcome the resolution limitations, a technique known as quantum optical coherence tomography (QOCT) has been proposed to exploit the automatic dispersion cancellation involved in the two-photon interference effect [48]. Moreover, for the same bandwidth, QOCT benefits from an extra factor of 2 in resolution compared to classical OCT. The experimental configuration of QOCT would be similar to that presented in figure 2, where the sample is introduced in one of the arms of the two-photon interferometer and coincidence counts

are recorded while varying the path of the other arm using a variable delay stage. Not long after its proposal, QOCT was experimentally demonstrated, achieving an improvement in resolution by a factor of 5 compared to OCT [49]. Further experimental demonstrations of QOCT have also been reported, where micron-sized features are detected even for the case of biological samples [50–52]. Finally, although QOCT offers potential advantages in terms of resolution, new challenges appear, such as low signal and signal artefacts. Thus, new techniques are being investigated in order to exploit the full potential of QOCT [53–56]. An example of a 3-dimensional image taken via QOCT for the skin of an onion coated in gold is shown in figure 3; this result indicates a resolution of 1 μm .

2.3. Quantum metrology

Finally, another field of research where the HOM effect plays an essential role for precision measurement is *quantum metrology*, where quantum resources, such as entanglement and non-classical states of light, are used to achieve higher precision on the measurement of a physical property [58, 59]. The most well-known class of useful states for quantum metrology is the N00N states [24], given by,

$$|\psi_{\text{N00N}}\rangle = \frac{1}{\sqrt{2}} (|N\rangle_a |0\rangle_b + |0\rangle_a |N\rangle_b). \quad (10)$$

Here, $|N\rangle$ represents N photons in the Fock basis.

For the trivial case of $N = 1$, such state is realized by sending a single photon through a 50:50 BS. For the case of $N = 2$ [60, 61], we recognize the state from equation (4) where two indistinguishable photons are made incident onto both input ports of a 50:50 BS, resulting in HOM interference. Thus, one can already appreciate the importance of the HOM effect in quantum metrology relying on the entanglement of multi-photon states. The resolution in space and phase is enhanced by a factor of N , i.e. scales as $1/N$. Thus, in order to achieve the fundamental quantum limit, also known as the Heisenberg limit, for phase sensitivity, one must consider high photon number N00N states. Several schemes have thus

been proposed to achieve high photon number N00N states experimentally [62–65] along with experimental demonstrations [66–75], where most of these schemes are in the spirit of the two-photon, or more generally multi-photon, interference set by the HOM effect.

3. Quantum state analysis

In the previous section, we have reviewed several experiments where the two-photon interference effect can be taken advantage of in order to perform precision measurements in terms of timing or phase sensitivity. Another case in which the two-photon interference is of paramount importance is the analysis of quantum states, such as pairs of indistinguishable and entangled photons. In particular, the measurement of the HOM visibility is an invaluable diagnostic tool to characterize single photon sources and states. Furthermore, Bell state measurements are the gold standard for experimentally measuring maximally entangled states.

3.1. Mode distinguishability

At the heart of the HOM effect, there is the concept of distinguishability of the input photons. In other words, two photons are said to be indistinguishable if they are in the same mode of the electromagnetic field, i.e. polarization, time, frequency, position and momentum. In a two-photon interference experiment, maximal interference occurs when the input photons are indistinguishable at both input ports of the BS. The level of indistinguishability is typically determined using the HOM interference visibility, \mathcal{V} , given by,

$$\mathcal{V} = \frac{C_{\max} - C_{\min}}{C_{\max}}, \quad (11)$$

where C_{\max} and C_{\min} correspond respectively to the maximal and minimal coincidence count rates at the output of the BS by varying the arrival time of one of the input photon, see figure 2(b). Indeed, the HOM visibility has been used to characterize the level of mode indistinguishability for a wide range of single photon sources, i.e. SPDC [76, 77], quantum dots [78–82], atomic vapours [83–87], nitrogen-vacancy centres in diamond [88–90], trapped ions [91], trapped neutral atoms [92, 93], and molecules [94, 95]. The experimental realization of indistinguishable single photon sources with high purity is a crucial component for engineering large-scale entangled quantum states from independent sources, as will be seen in forthcoming sections.

3.2. Bell state measurements

In general, the discrimination of Bell states with linear optics comes with fundamental limitations. For example, if we use exclusively linear optics and no other ancillary modes, we are bound to a 50% discrimination success rate [96]. Higher success rates can be achieved with nonlinear optics [97], entanglement in auxiliary modes [98, 99], or feed-forward techniques [100]. The simplest implementation uses only one interference at a single BS and two detectors. We start with two maximally entangled modes in the Bell basis, $|\Psi^\pm\rangle_{ab}$ and $|\Phi^\pm\rangle_{ab}$ from

equations (5) and (6), respectively. Recall that the BS transforms the Bell states according to equation (7), explicitly given as,

$$\begin{aligned} |\Psi^+\rangle_{ab} &\xrightarrow{\text{BS}} \frac{1}{\sqrt{2}} (|1\rangle_{c,H}|1\rangle_{c,V} - |1\rangle_{d,H}|1\rangle_{d,V}), \\ |\Psi^-\rangle_{ab} &\xrightarrow{\text{BS}} \frac{-1}{\sqrt{2}} (|1\rangle_{c,H}|1\rangle_{d,V} - |1\rangle_{c,V}|1\rangle_{d,H}), \\ |\Phi^\pm\rangle_{ab} &\xrightarrow{\text{BS}} \frac{1}{2} (|2\rangle_{c,H} \pm |2\rangle_{c,V} - |2\rangle_{d,H} \mp |2\rangle_{d,V}), \end{aligned} \quad (12)$$

where $|N\rangle_{p,s}$ is N photons in the path p with polarization s . Again, we see the bunching of the HOM effect acting on the last two states. In the first case, both photons end up in the same detector, but they have opposite polarization; in the second case, we have one photon per detector, and in the last case they also reach the same detector, but they have the same polarizations. We cannot distinguish the last two states, $|\Phi^\pm\rangle$, from each other with a simple pair of photon detectors; hence, the success rate of 50%. As anticipated, this figure can be improved by supplying some additional entangled modes. As outlined in [101], an example can be to arrange four BSs so that we interfere the original state with another entangled ancillary pair of modes first, and then each of the two pairs of output modes goes through a simple Bell state analyzer. In this way, we can distinguish one of the two states that we could not distinguish before, raising the success rate to 75%. It is possible to combine N interferences and raise the success rate to $1-2^{-N}$.

4. Quantum communication

A major and growing part of quantum technologies is the field of quantum communications and quantum cryptography [102, 103]. Carriers of information made of single quanta of energy, such as photons, possess a surprisingly large potential for secure communications. The Heisenberg uncertainty principle and the no-cloning theorem [104] are the basis of security when encoding information on single photons, since any type of eavesdropping results in disturbances of the photonic quantum states. Another key physical principle that is at the heart of quantum communications is entanglement [22]. In particular, quantum cryptography takes an elegant form when explained in terms of entanglement-based schemes [23] and can further simplify security analyses [105]. Beyond quantum cryptography, many quantum communication schemes—such as entanglement swapping [106], quantum teleportation [107], and dense-coding [108]—are also based on the concept of entanglement.

In the following section, we review the role of the two-photon interference effect in established schemes such as quantum teleportation and entanglement swapping. Subsequently, we review recently introduced quantum cryptographic schemes that are based on the two-photon interference effect. In particular, the *measurement-device-independent* [109, 110] and the passive *round-robin differential phase-shift* [111] QKD protocols are considered, which are milestones for the emerging field of *practical* QKD.

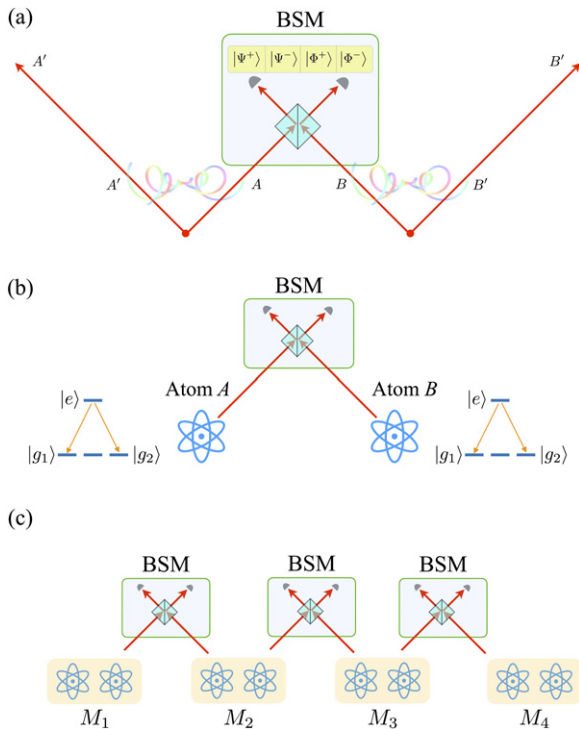


Figure 4. Schematic of performing entanglement swapping. (a) Given two entangled systems AA' and BB' , A and B are made to interfere at a 50:50 BS in the form of a Bell state measurement (BSM). Thus, A' and B' are consequently entangled based on the outcome of the BSM. (b) A BSM is performed on two photons created from two separate excited atoms. Similar to (a), the two atoms become entangled based on the outcome of the BSM. (c) A quantum repeater scheme with four memories in which each memory contains two separate atoms. Following (b), a BSM is made on two photons from neighbouring memories to entangle the neighbouring atoms. By cascading such a process, the entanglement can be distributed over long distances.

4.1. Teleportation and entanglement swapping

The idea of entanglement swapping is to start with a pair of entangled systems, AA' and BB' , and to measure systems AB in the Bell basis, with the consequence of leaving systems $A'B'$ entangled with each other. This is entanglement swapping in a nutshell. The way we can achieve it is indeed to perform a Bell state measurement, whose outcome determines in which Bell state the other two systems are left, see figure 4(a).

For example [112], consider a single trapped excited atom with a degenerate ground state corresponding to two distinct photon polarizations, as shown in figure 4(b). In such a way, when the atom emits a photon, the atom-photon state is $\frac{1}{\sqrt{2}}(|g_1, H\rangle + |g_2, V\rangle)$, where g_1 and g_2 are the two orthogonal ground states. When there are two such events from two different atoms (from different cells), the emitted photons can be interfered at a BS to perform a linear optical Bell state measurement, as discussed in the previous section. If successful, this procedure has swapped the entanglement from being between each atom and its photon to being between the two atoms alone. We have thus created an entangled state of two atoms, which will display non-local correlations as one can verify for example by violating Bell's inequalities

[113]. This idea can be applied to other domains as well, for example to entangle a pair of transmon qubits by interfering two microwave photons at a microwave BS junction [114].

Another domain of utilization is for quantum repeaters [115]: the so-called 'two-way architecture' works by having quantum memories evenly distributed along a communication channel, each memory hosting two atoms that emit photons as described above, one forwards and one backwards along the channel, see figure 4(c). Mid-way between two memories M_1M_2 sits a Bell state analyzer that measures the two photons coming from M_1 and M_2 in the Bell basis. If the measurement is successful, we have entangled a pair of atoms, one in M_1 and one in M_2 . As soon as this procedure is successful between the second atom in M_2 and an atom in M_3 , the memory M_2 can itself measure its two atoms in the Bell basis, with the consequence of entangling a pair of atoms, one in M_1 and one in M_3 . One can continue with this protocol until the first and the last memories are entangled, and we have thus effectively obtained an entangled pair of atoms among potentially very distant locations [116]. These can then be used to perform any kind of protocol, from QKD to distributed quantum computations [115].

4.2. Measurement device independent QKD

In theory, QKD promises the exchange of secret information, where the security relies on fundamental physical principles. Nevertheless, practical implementations do not necessarily follow the assumptions made in the security proofs. Thus, security loopholes have, early on, been recognized to pose a threat to the security of realistic QKD implementations [117, 118]. For instance, several side channel attacks have been demonstrated experimentally, showing the vulnerability of the commercial QKD systems under study [119, 120]. In order to overcome these security issues, several solutions have been proposed. One such solution is known as the full device independent QKD [121, 122], where the security can be proven without any knowledge of the devices used in the implementation. However, this scheme yields very low secret key rates, and is highly impractical due to several stringent requirements such as near unity detection efficiencies. In order to overcome the impracticality of this scheme, the measurement-device-independent (MDI) QKD protocol has been proposed [109, 110], where all detector side channels attacks are now removed. In contrast to the full device independent scheme, MDI QKD protocol still necessitates the assumptions of Alice's and Bob's states generation to be perfect, which is still reasonable for current implementations.

The two-photon interference and Bell state analysis are central concepts in MDI QKD. The protocol goes as follows: Alice and Bob randomly prepare their individual photons in a particular state, then distribute their photons to a third untrusted partner, named Charlie. Upon receiving Alice's and Bob's photons, Charlie performs a Bell state measurement by making each photon incident on a BS. The two photons are made to arrive simultaneously on the BS, in order to observe two-photon interference. Finally, Charlie publicly announces the result of his Bell state measurement, allowing Alice and Bob to establish a shared raw key. Usual classical post-processing,

such as error correction and privacy amplification, is then applied in order to obtain a secure secret key between Alice and Bob. The MDI QKD protocol has been experimentally demonstrated using time-bin phase-encoding [123], and polarization encoding [124]. Moreover, the MDI scheme has also been demonstrated over long distances through optical fibres [125, 126], showing the feasibility of the protocol and its potential for unconditional security. In the aforementioned implementations of MDI QKD, to achieve high secret key rates, attenuated laser pulses were employed along with the decoy state protocol [127]. In order to achieve an optimal HOM interference, the attenuated lasers are phase randomized, achieving a maximum HOM visibility of 1/2. A heralded single photon source achieving a unity HOM visibility would lead to a higher secret key rate per transmitted photon. Furthermore, a continuous variable MDI QKD protocol has also been introduced theoretically and experimentally implemented using coherent states and continuous variable Bell detection, which can lead to high bit rates [128].

4.3. Passive round-robin differential phase shift QKD

Another milestone in QKD is the round-robin differential-phase shift (RRDPS) protocol [129]. An important task in any practical QKD implementation is the assessment of the information leakage to an adversary eavesdropper. By determining this quantity, one may then perform the appropriate amount of classical post-processing to the raw key shared between Alice and Bob. However, determining the amount of information leakage requires active monitoring of the quantum bit error rate, or other quantities such as interference visibilities. This stringent requirement may render several QKD implementations impractical or lower its key rate efficiency. The RRDPS protocol removes the requirement for signal disturbance monitoring by bounding the amount of information leaked to the eavesdropper, where the bound depends entirely on Alice's generation stage. Hence, the RRDPS scheme is another major step towards practical implementation of unconditionally secure quantum communication systems.

Several realizations of the RRDPS protocol have recently been demonstrated experimentally using time-bin phase encoding [130–133] and using transverse spatial modes [134]. Although a single bit of information per transmitted pulse is encoded, the RRDPS QKD can be considered as a high-dimensional protocol. Dimensions ranging between 5 and 128 have been achieved in the time-bin configuration using interferometers with variable delays. In particular, the security of the RRDPS protocol is largely enhanced when considering large dimensions; therefore, it is worth exploring different implementations achieving larger dimensions. In order to overcome the difficulties in achieving stable variable-delay interferometers, a passive version of the RRDPS QKD was proposed [111]. In this scheme, the two-photon interference is exploited to achieve extremely large dimensions such as 10^5 . Instead of measuring the interference of a train of pulses at Bob's stage, Bob generates a reference pulse train, and sends Alice's and his state to a BS. By using such a configuration,

Bob takes advantage of the phase stability of the two-photon interference effect. Finally, it has recently been shown that the passive RRDPS protocol could also be extended to other high-dimensional QKD protocols [135].

The passive RRDPS QKD is another demonstration of the advantage of using the two-photon interference effect in quantum communications protocols. As a result, such a configuration typically yields larger security, better stability, and faster communications.

5. Quantum state engineering

One of the necessary ingredients for quantum technologies is the ability to manipulate quantum systems to bring them to the desired state. For example, in metrological applications, certain states are more sensitive than others to the effect that we want to measure; or in quantum computation, the system should be initialized in a subspace that offers protection from errors. Furthermore, in light of the Choi–Jamiołkowski isomorphism which allows us to associate a bipartite state to a quantum channel [136, 137], generating the desired quantum states also has consequences on our ability to implement full quantum channels through the technique of gate teleportation.

In this section, we describe some of the achievements of quantum state engineering: the measurement and generation of entangled states, quantum cloning, and the technique of state merging—all through the lens of the HOM effect.

5.1. Entanglement engineering

Starting from a highly entangled pair of particles, such as the photon pairs generated in SPDC, it is possible to engineer the state to one's needs using the HOM effect. Any input state of the BS with one photon in each input port can be written as $|\Psi\rangle = \sum_{i,j=1}^d c_{ij} |1\rangle_{a,i} |1\rangle_{b,j}$, with $|1\rangle_{p,k}$ representing one photon in path p with mode k . It is shown in [138] that this can be rewritten as a superposition of symmetric and antisymmetric Bell states $|\Psi\rangle = \sum_{i \neq j} \frac{c_{ij}}{\sqrt{2}} (|\Psi_{ij}^+\rangle + |\Psi_{ij}^-\rangle) + \sum_i c_{ii} |\Psi_{ii}^+\rangle$, where $|\Psi_{ij}^\pm\rangle = |1\rangle_{a,i} |1\rangle_{b,j} \pm |1\rangle_{a,j} |1\rangle_{b,i}$. Upon exiting the BS, the symmetric component, $|\Psi_{ij}^+\rangle$, of the input state will result in two photons being detected in one of the output ports, while the antisymmetric component, $|\Psi_{ij}^-\rangle$, will result in one photon being detected in each output port. Therefore, when conditioning on coincidence detection between the two output ports, the HOM effect acts as a filter for the antisymmetric component for any arbitrary high-dimensional input state.

A second example is a way of entangling photons with different frequencies [139]. The idea here is to create two pairs of photons and make a joint Bell state measurement, implementing what is known as 'entanglement swapping' (see section 4.1). The frequency difference $\Delta\omega$ generates a phase of $\exp(i\Delta\omega\Delta t)$ between the components, which will render the state mixed if unaccounted for because the detection time difference Δt is random. However, one can solve this issue either by postselecting on only the measurements that fall within a very narrow time window (but this reduces the total number

of successful measurements), or by recording the time difference and feed-forward a phase correction so that every single photon pair will have the same phase.

5.2. Universal optimal quantum cloning and NOT gate

Another application of the HOM effect is *quantum cloning*. Considering the well-known fact that quantum mechanics does not allow the possibility to clone an unknown state [104, 140], the ability to perform quantum cloning may seem counterintuitive. The key is that, in quantum mechanics, we are allowed to perform a task as long as we cannot use it to violate the linearity of the theory. The no-cloning theorem states that we cannot *always* clone an unknown state, which is indeed correct; however, this does not prevent us from creating a clone some of the time with random success. Optimal $1 \rightarrow 2$ cloning (i.e. two clones of one original state) of a qudit can be achieved with a fidelity of $F_{\text{cloning}} = \frac{1}{2} + \frac{1}{d+1}$ [27, 141–143].

For example, an arbitrary polarization qubit $|1\rangle_s = \alpha|1\rangle_H + \beta|1\rangle_V$, where $|\alpha|^2 + |\beta|^2 = 1$, can be optimally cloned using the HOM effect by interfering it on a BS with an ancilla that is in a maximally mixed polarization state $\hat{\rho} = (|1\rangle_s\langle 1| + |1\rangle_{s_\perp}\langle 1|)/2$, where s_\perp is the orthogonal polarization state. The total dimension of the system is $d + 1 = 3$, since the mixed state has dimension 2, while the arbitrary polarization qubit is an independent vector, adding an additional dimension. When the two photons exit through the same port, $2/3$ of the time they will have the same polarization state; while $1/3$ of the time, they will have orthogonal polarization states, $|1\rangle_s|1\rangle_{s_\perp}$. Overall, the cloning fidelity is then $F_{\text{cloning}} = \frac{2}{3} \times 1 + \frac{1}{3} \times \frac{1}{2} = \frac{5}{6}$.

Suppose we created the maximally mixed polarization state by using one of the photons from a maximally entangled singlet state. Then $2/3$ of the time, the other photon in the singlet state will have the orthogonal polarization of the cloned states, and $1/3$ of the time the same polarization. This effectively implements an optimal universal NOT gate [144, 145]—itself a non-unitary operation.

5.3. Quantum state joining

Quantum state joining is the process of transferring the state of two particles onto a third one (replacing its state). We thus require a particle to have enough degrees of freedom to accommodate the information of both incoming states. For example, when working with photons, this can be achieved by exploiting the spatial degree of freedom in addition to polarization, but one could also use the frequency/time degree of freedom.

The Knill–Laflamme–Milburn (KLM) linear optical implementation of the CNOT quantum gate, which will be discussed in detail in section 6.1, plays the key role for achieving quantum state joining. Experimentally, quantum state joining has been achieved for the polarization state of two photons, in which the information was transferred onto a third single photon by exploiting the fact that a single particle can occupy different spatial modes and polarizations [146]. This process is probabilistic and requires an ancilla state, with a success

probability of $1/32$, or $1/8$ if a suitable feed-forward is used. Explicitly, the polarization state of two particles,

$$\begin{aligned} |\phi\rangle_I \otimes |\psi\rangle_{II} &= (\alpha|1\rangle_{IH} + \beta|1\rangle_{IV}) \otimes (\gamma|1\rangle_{IHH} + \delta|1\rangle_{IIV}) \\ &= \alpha\gamma|1_H, 1_H\rangle + \beta\gamma|1_H, 1_V\rangle \\ &\quad + \alpha\delta|1_V, 1_H\rangle + \beta\delta|1_V, 1_V\rangle, \end{aligned} \quad (13)$$

where $|1_s, 1_{s'}\rangle = |1\rangle_{Is} \otimes |1\rangle_{IIs'}$, respectively, can be joined onto the state of a third single photon,

$$|\varphi\rangle_{III} = \alpha\gamma|1\rangle_{\cdot 0\cdot} + \beta\gamma|1\rangle_{\cdot 1\cdot} + \alpha\delta|1\rangle_{\cdot 2\cdot} + \beta\delta|1\rangle_{\cdot 3\cdot}. \quad (14)$$

Here, the subscripts $\{‘0’, ‘1’, ‘2’, ‘3’\}$ represents a 4-dimensional logical basis, e.g. path-polarization or OAM. This scheme relies on the interaction of two photons, which would require nonlinear optics. The inverse process to joining states, known as quantum state splitting, is such that the information on a ququart state (for the above experiment) is split onto two photonic qubits [147].

6. Quantum computation

After having covered a few examples of engineering quantum states, we can now move on to engineering the dynamics of a system. In particular, we want to focus on those dynamics that can be considered a ‘computation’ on quantum data. Of course, a complete treatise of quantum computing would require much more space than that of this section, so our aim here is to summarize the main idea and then show how the HOM effect can be harnessed to perform some meaningful quantum state processing.

6.1. Linear quantum computing

Universal quantum computation can be achieved with linear optics, post-selection, single photon sources and detectors, and feed-forward, as was proposed by the KLM protocol [100]. Here, qubits are defined in the dual-rail encoding, i.e. the computational states are defined as a single photon that occupies one of a pair of optical modes. In our notation, a single photon qubit can be written simply as $|\phi\rangle = \alpha|0, 1\rangle + \beta|1, 0\rangle$, where the first and second labels in each ket corresponds to the number of photons in each rail. The logical qubits in the dual-rail encoding could, for example, be $|‘0’\rangle := |1, 0\rangle$ and $|‘1’\rangle := |0, 1\rangle$. Single qubit gates are then optical components that couple pairs of modes, such as a BS. For two-qubit gates where interaction is required, the HOM effect is relied heavily upon. Two such gates are the control-Z (CZ) and control-NOT (CNOT) gates, which are the main components for universal quantum computation.

The two-qubit CZ gate performs the following operation,

$$|q_1, q_2\rangle \rightarrow (-1)^{q_1 q_2} |q_1, q_2\rangle, \quad (15)$$

where q_1 and q_2 are the control and target logical qubits, respectively, taking values of ‘0’ or ‘1’. It was found that a CZ gate can be constructed using two 50:50 BS and two so-called nonlinear sign (NS) gates [100], see figure 5(a). An

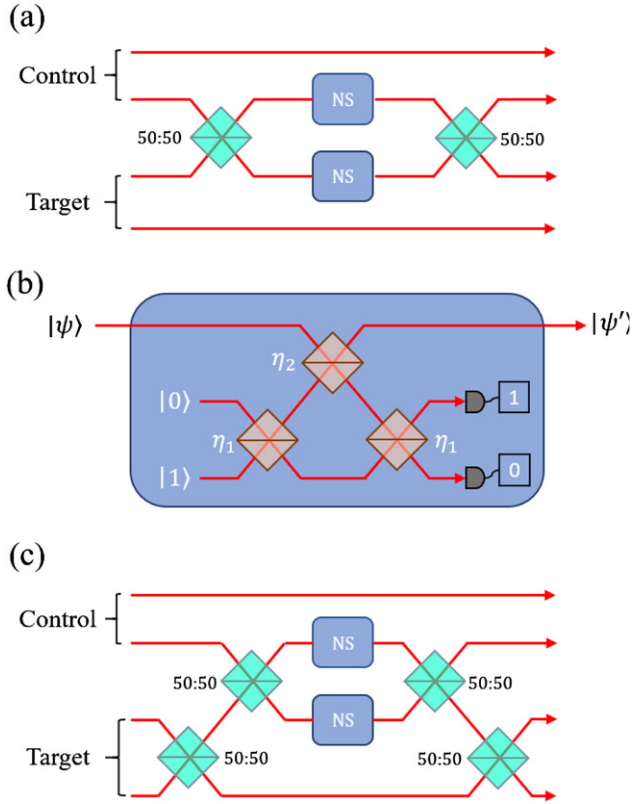


Figure 5. Schematic of photonic quantum gates. (a) Control-Z gate. (b) Nonlinear sign gate with $\eta_1 = 1/(4 - 2\sqrt{2})$ and $\eta_2 = 3 - 2\sqrt{2}$. (c) Control-NOT gate.

NS gate applies a π phase shift to only the two-photon Fock state, i.e.

$$|\psi\rangle = \alpha|0\rangle + \beta|1\rangle + \gamma|2\rangle \xrightarrow{\text{NS}} |\psi'\rangle = \alpha|0\rangle + \beta|1\rangle - \gamma|2\rangle. \quad (16)$$

As shown in figure 5(b), the NS gate uses two ancillary modes (vacuum and a single photon), three BS with transmission amplitudes of $\eta_1 = 1/(4 - 2\sqrt{2})$ and $\eta_2 = 3 - 2\sqrt{2}$. The NS gate is successful, i.e. equation (16) occurs, when the photon number resolving detectors detect 1 and 0 photons, respectively. This post-selection process renders the NS gate to be probabilistic, with a success probability of $p_{\text{NS}} = 1/4$ for an arbitrary input state without feedforward. The upper bound for the NS gate was found to be $1/2$ [148]. Variations of the NS gate have been reported: one proposal shows the possibility to implement it using only two BS but with slightly lower success probability of $(3 - \sqrt{2})/7$ [149]; other schemes with again two ancillary photons with success probabilities $1/5$ [150] and $1/4$ [151]. It is also possible to implement the NS gate in the polarization basis, wherein polarization rotations are used instead of the variable BS; this also has a success probability of $(3 - \sqrt{2})/7$. Overall, we see that the CZ gate heavily relies on the HOM effect, the output depending on whether the control and target photons bunched or not. Since two NS gates are required, the total success probability of this CZ gate is $p_{\text{CZ}} = p_{\text{NS}}^2$. The most efficient CZ gate has a success probability of $2/27$, utilizing two single photon ancillary modes and only four BS [152].

The CNOT gate performs the operation $|q_1, q_2\rangle \rightarrow |q_1, q_2 \oplus q_1\rangle$, where \oplus denotes addition modulo 2. In this way, the target qubit is flipped if and only if the control qubit is '1'. The implementation of the CNOT gate is similar to that of the CZ gate in that it requires two NS gates; however, two additional 50:50 BS are required acting on the target qubit [153], as shown in figure 5. Again, since the CNOT gate is based around the NS gate, it is a probabilistic process with success probability $p_{\text{CNOT}} = p_{\text{NS}}^2 = 1/16$.

It is possible to achieve a useful quantum computation without resorting to a universal quantum computer. In this case, it is sufficient to have a device that performs a single algorithm. There are several examples of specific quantum optical implementations that rely on the HOM effect, to list a few: solving systems of linear equations [154, 155], computation on encrypted data [156], computing discrete and fractional Fourier transform [157], and computations on a single spatial mode (using temporal modes) [158].

Once the experimentation phase of a new technology becomes mature enough, it is followed by a phase of better production methods which may include miniaturization into embedded devices. This is a trend that quantum optical technologies are experiencing at the moment. Waveguides in photonics chips allow for higher portability, higher cost efficiency, and higher robustness [159, 160].

6.2. The SWAP test

The HOM effect is colloquially referred to as a test for the distinguishability between two photons: if we witness a coincidence, the two photons had different states. Similarly, the SWAP test is a quantum computing primitive operation that tests for the inequality between two quantum states. Perhaps surprisingly, the analogy between them goes all the way down to formal equivalence: the HOM effect is an optical implementation of the (destructive) SWAP test [161]. In this section, we will explain this formidable equivalence.

Let us analyse what occurs in the SWAP test, see figure 6 for the circuit. At the input, we have two states $|\phi\rangle$ and $|\psi\rangle$, and an ancillary logical qubit initialized in $|0\rangle$. The Hadamard (H) gate converts the state $|0\rangle$ into a superposition $\frac{|0\rangle + |1\rangle}{\sqrt{2}}$ (and the state $|1\rangle$ into $\frac{|0\rangle - |1\rangle}{\sqrt{2}}$). The controlled-SWAP (CSWAP) gate swaps the states $|\phi\rangle$ and $|\psi\rangle$ if the ancillary qubit is in state $|1\rangle$, and does nothing otherwise. The evolution of the input throughout the SWAP test is,

$$\begin{aligned} |0\rangle |\phi\rangle |\psi\rangle &\xrightarrow{\text{H}} \frac{|0\rangle + |1\rangle}{\sqrt{2}} |\phi\rangle |\psi\rangle \\ &\xrightarrow{\text{CSWAP}} \frac{|0\rangle |\phi\rangle |\psi\rangle + |1\rangle |\psi\rangle |\phi\rangle}{\sqrt{2}} \\ &\xrightarrow{\text{H}} \frac{|0\rangle(|\phi\rangle|\psi\rangle + |\psi\rangle|\phi\rangle) + |1\rangle(|\phi\rangle|\psi\rangle - |\psi\rangle|\phi\rangle)}{2}. \end{aligned} \quad (17)$$

In terms of the measurement outcome, if $|1\rangle$ is measured, we can confirm that the two input states are different; however, if the outcome is the state $|0\rangle$, they may or may not be equal. Equivalently in terms of the states $|\phi\rangle$ and $|\psi\rangle$, if they are identically equal, the second term in the last line of equation (17)

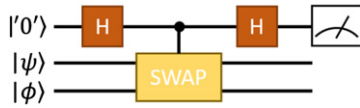


Figure 6. SWAP test. The quantum circuit implementing the SWAP test on the states $|\psi\rangle$ and $|\phi\rangle$. A measurement of ‘1’ implies that the states are different, while a measurement of ‘0’ is inconclusive.

vanishes and the outcome of the measurement must be $|0'\rangle$ with probability 1. However, if they are not equal, either of the two possible outcomes could be measured. If we demonstrate their inequality, we say the states ‘fail’ the test; otherwise, we say that the states ‘pass’ the test. As mentioned above, passing the test does not mean that the states are equal: we can only say that the more copies of the initial pair pass the test, the more certain we are about their equality.

From equation (17), we can find the probability for passing the test is $(1 + |\langle\phi|\psi\rangle|^2)/2$, and consequently the probability of failing the test is $(1 - |\langle\phi|\psi\rangle|^2)/2$. This means that the more similar the two states are, the harder it is to demonstrate their inequality. For two maximally distinguishable (orthogonal) states, the overlap is 0 and $P = 1/2$, while for maximally indistinguishable states the overlap is 1 and the probability to pass the test is also 1. This justifies the notion that we are certain that the states are not equal if they fail the test.

The eigenstates of the SWAP operator are the Bell states: three Bell states correspond to the eigenvalue +1 (the symmetric subspace), and one corresponds to the eigenvalue −1 (the singlet state, i.e. the antisymmetric subspace). This suggests that one could also implement a *destructive* SWAP test by measuring directly the two systems in the Bell basis. In order to make a full equivalence with the HOM effect, we need to get rid of the ancillary qubit. This can be done by exploiting the observation that the SWAP test projects the two input states onto the symmetric/antisymmetric subspaces of the space of states, which is what a Bell state measurement does. For the two-dimensional case, we can implement a Bell state measurement with a single BS followed by a detector in each output port, which is equivalent to a *destructive* SWAP test in the sense that the states get measured and are not available afterwards. In higher dimensions, one needs the equivalent circuit for projecting onto the symmetric/antisymmetric subspaces. This is sufficient to conclude the full analogy between the HOM effect and the SWAP test.

7. Generalization to multipartite and multimode systems

So far, we have only discussed two-photon interferences appearing in a 2-input/2-output device, i.e. a BS, just as it was envisioned in the original experiment by Hong, Ou and Mandel. However, the property of multiphoton interference is not limited to this rather simple (and yet powerful) case, but it can be generalized to more particles in more complicated BS networks with multiple-input and multiple-output ports, i.e. so-called multiports. Although such studies have been started

soon after Hong, Ou and Mandel’s seminal paper [162–164], the recent development of more efficient photon sources and the shift to integrated quantum optics experiments has led to a revival and extension of these investigations. We refer the reader to [165] for a comprehensive review of multi-photon interference.

7.1. Three-photon interferences in a Bell-tritter

It is suggestive to generalize the two photon BS arrangement at first to a three photon and three-mode analog to a BS, a so-called tritter [166, 167]. Similar to the two photon HOM-interference, three photons can interfere in a tritter if they are indistinguishable. In general, the output probability distribution of the three photons depends on the input distribution as well as the exact unitary transformation of the tritter. Although any unitary transformation between the input and output modes might be possible and of some interest [163], it is instructive to look into the simple case of a so-called Bell-tritter [166, 167], which redistributes the three incoming photons to the three output ports in an unbiased way. The ideal unitary transformation U^{tritter} of a Bell-tritter is mapping the input field operators a_i^\dagger to the output field operators $b_i^\dagger = \sum_j U_{ij} a_j^\dagger$ and can be described [168] by,

$$U^{\text{tritter}} = \frac{1}{\sqrt{3}} \begin{pmatrix} 1 & 1 & 1 \\ 1 & e^{i2\pi/3} & e^{i4\pi/3} \\ 1 & e^{i4\pi/3} & e^{i8\pi/3} \end{pmatrix}. \quad (18)$$

Bell-ports have been discussed theoretically since many years in connection to multipartite and high-dimensional quantum information [163, 166, 167]. They have also been experimentally realized with fused optical fibres [164] and more recently with passive [168] and active integrated waveguide circuits [169]. Although tritters have been used to demonstrate quantum features in the two-photon regime [164, 169, 170], only recently have three-photon HOM coalescences been observed [168, 171]. Analog to the two-photon HOM effect, if three indistinguishable photons are sent into the three input ports, not all possible output-distributions will be realized. As can be seen in figure 7(a) for a three-dimensional Bell-port, bosonic coalescence leads to only 4 out of 10 possible output distributions. By making the photons pairwise distinguishable, e.g. by delaying independently two photons, one can map a probability surface with non-trivial features (see figure 7(b)). This surface can be seen as the three-dimensional extension to the 2-dimensional HOM interference dip [168]. Importantly, the complex features of three-partite interference experiments were also discussed in terms of quantum metrology and phase sensing to enhance precision [172].

While these results can be seen as a direct extension to the standard two-photon HOM effect, another recent experiment demonstrated that there are additional features unique to multipartite interferences [171]. In contrast to the two-photon case, where the interference is solely dictated by the distinguishability of the two photons, the interference becomes more complex when more particles are involved. For three photons for example, an additional collective phase is required to describe

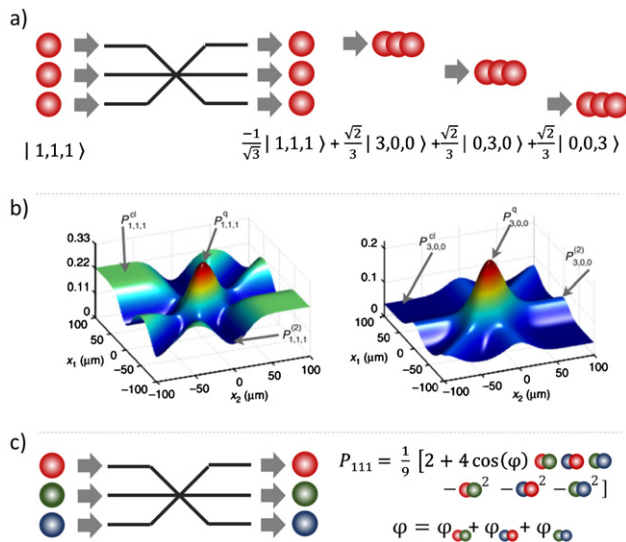


Figure 7. Three photon interference in a tritter. (a) Three photon analog to the original HOM experiment. If three indistinguishable photons are sent to a Bell tritter (see unitary (18)), only 4 out of 10 possible outcome are allowed. (b) Theoretical output probabilities for detecting all photons in different output ports $P_{1,1,1}$ (left) and the same output port $P_{3,0,0}$ (right) as a function of the delay of the input photons. Reprinted by permission from Springer Nature Customer Service Centre GmbH: Nature Communications. [165] © 2013. (c) If the photons are partially distinguishable (depicted by the different colours), the output probability $P_{1,1,1}$ also depends on the triad phase φ , which is the sum of pairwise phase differences of the photons. Reprinted figure with permission from [168], Copyright (2017) by the American Physical Society.

the photons' scattering behaviour [173–175]. This so-called triad phase is the sum of the three relative phases between pairwise inputs (see figure 7(c)) and only effects the outcome if the photons are partially distinguishable. It leads to a change in the detection probabilities when all three photons are detected in separate output ports and does not affect the bi-photon transmission probabilities. Thus, it has to be considered a genuine three-photon interference effect with no analog in the standard HOM experiment. Furthermore, similar concepts and results, such as a zero-transmission law for various output distributions, can also be generalized to n bosons sent in the n ports of a Bell-multiport [176–179].

7.2. Multiphotons in general multiports

After this initial generalization step, one can extend the discussion by enlarging the number of modes of the multiport device and by increasing the number of involved particles. The increasing complexity opens a myriad of different effects, which have been or will be studied and that are all relying on the interference of two or more particles. When two particles for example are sent into a multiport, e.g. multimode waveguide [180, 181], multimode fibre [182] or integrated waveguide structures [183], the transmission can be described as a complex bi-partite quantum walk that gives rise to interesting quantum correlation patterns [184, 185], can be used to perform quantum simulations [186, 187] or can probe the statistics in quantum walks [188].

As discussed in the last paragraph, if more than two photons are interfered, a probability surface or coincidence landscape can be investigated [189], which is useful to probe indistinguishability or to predict the complex device's quantum behaviour [190]. Recently, it has been shown both theoretically and experimentally that the temporal multimode structure of quantum states directly affects four-photon interference [191]. Interferences of many bosons in complex network structures have also found various applications in quantum information science. Most recently, a multiphoton interference in a multiport has enabled the first quantum teleportation of a high-dimensional quantum state [192]. The procedure for high-dimensional quantum teleportation is very similar to the one for qubits; however, a high-dimensionally entangled pair has to be shared between the two parties first. In addition, depending on the dimensionality of the teleported state, $d-1$ ancillary photons are required to perform the high-dimensional Bell-state measurement. In the experiment, a three-dimensional quantum state was teleported using one additional ancillary photon. After appropriate postselection, the three-dimensional quantum state was found to be teleported to the photon, which was initially a part of the entangled pair. The complex interference of multiple photons in multiports cannot only be used in teleportation schemes, it also enables the generation of multi-partite entanglement [193].

Moreover, the enormous complexity of the underlying physics is nicely illustrated in terms of the so-called boson sampling problem [194, 195]. It has been shown that calculating the output probability distribution for a sufficiently large number of photons interfering in a large multiport arrangement is exponentially hard to solve classically, and as such it is considered to be a promising candidate to show quantum supremacy. In addition, it is also suggested that this challenges a fundamental principle of computer science, namely the extended Church–Turing thesis. Because of the complexity of this topic and as well as the enormous attention and progress that has been done over the last few years [196–203], boson sampling would justify a review on its own and we refrain from discussing it in more detail. Instead, we conclude with the note that, in all boson sampling tasks, multi-photon as well as multimodal interferences, i.e. generalizations of the original HOM idea, play a crucial role.

8. Implementations in non-photonic systems

While most of the experiments studying and utilizing the HOM interference use single photons and follow the original proposal, it has also been investigated extensively with other quantum systems. In this section, we will discuss the cases of plasmons, phonons, atoms, and electrons.

8.1. Plasmons

Using plasmons as quantum carriers has been an increasingly popular field in quantum science that pushed forward the advantages of light–matter interactions at the nano-scale and investigates its quantum physical features. So-called surface plasmon polaritons (SPP) are the quanta of the surface plasma

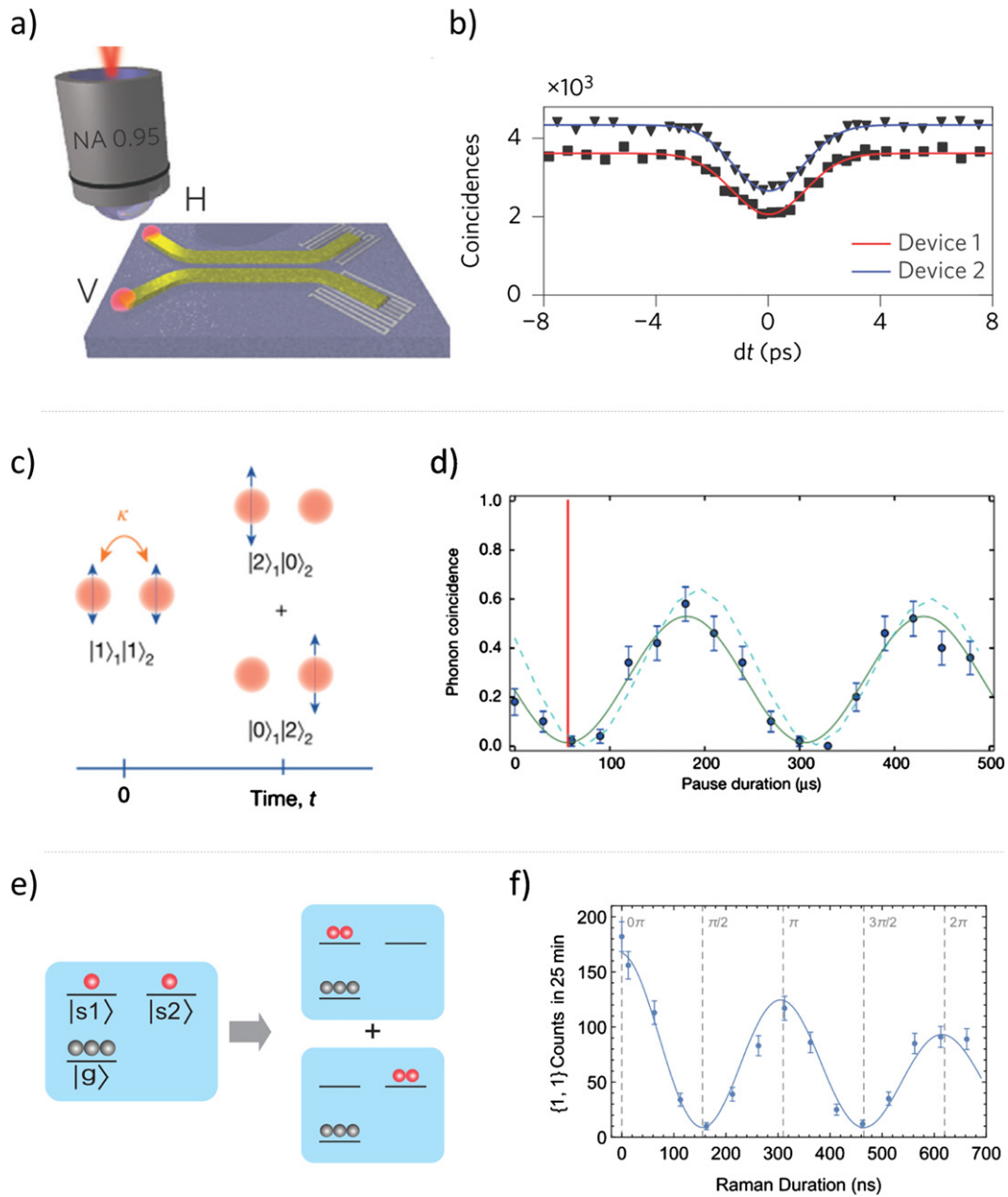


Figure 8. Non-photonic HOM interference. HOM interference with plasmons (a), (b) Reprinted by permission from Springer Nature Customer Service Centre GmbH: Nature Nanotechnology. [205] © 2013, phonons (c), (d) Reprinted by permission from Springer Nature Customer Service Centre GmbH: Nature. [206] © 2015 and collective excitations (e), (f) Reprinted figure with permission from [207], Copyright (2016) by the American Physical Society. (a) Two plasmons are excited by two single photons, brought to interference by a waveguide beam splitter and detected on chip by a superconducting detector. (b) The coincidence counts between the two detectors as a function of the delay of one input photon show the expected HOM dip. (c) Two phonons are excited on each site of a two-ion crystal and are allowed to hop to the neighbouring ion. After a specific time t corresponding to a 50:50 beam splitter, the phonons are only found at one of the two ions. (d) Phonon coincidence deduced from the read-out of the internal state as a function of waiting time until the read out is performed. The red vertical line depicts the time of 50% hopping probability. (e) Rb atoms were collectively excited into two different Zeeman levels and coupled through a stimulated Raman pulse. If pulse length corresponds to a 50:50 coupling, the excitations are bunched together. (f) Coincidence measurements of the two different excitations show a clear dip for multiple of $\pi/2$ coupling ratios.

wave, analog to photons in the electromagnetic field. Their theoretical prediction dates back to the 1950s; however, the experimental investigations in the quantum realm has only been started recently (for a more detailed review about quantum plasmonics, we refer the interested reader to [204, 205]). Because SPPs are described as quasiparticles with a bosonic nature, they were also expected to bunch in an HOM-type

experiment. While first experiments involving HOM interference only tested the persistence of the indistinguishability when photons are coupled to plasmons and back to photons [206, 207], actual plasmonic bunching was experimentally observed in 2013 [208]. The experiment was performed in very close analogy to integrated photon experiments using plasmonic waveguides to guide the plasmons

to a dielectric bi-directional coupler acting as the 50:50 BS (see figure 8(a)). At first, photon pairs were generated from an SPDC source, which were then transferred to SPPs and brought to interference. After mixing on the BS, the plasmons were directly detected using on-chip superconducting single plasmon detectors. Analog to photon experiments, the arrival time of one plasmon at the BS was scanned by means of a photonic delay line while the coincidence counts were registered. Although the observed dip had only a visibility of 0.43 ± 0.02 (see figure 8(b)) and thus below the classical limit of 0.5, the result is a nice indication of a two plasmons quantum interference. Moreover, soon after this initial demonstration, different experiments using different plasmonic configurations, and off-chip photon detection schemes achieved visibilities far beyond the classical limit up to 0.95 [211–214], thus fully certifying the quantumness of the two plasmon interferences. Moreover, in another recent study, it was shown that the usually deleterious losses associated with plasmonic systems might be turned into an advantageous feature when the nanostructures are carefully tuned. At the plasmonics BS, anti-coalescence or non-linear absorption can be observed [215]. Since two plasmon HOM interference is now well-established, it can be considered one of the building blocks of future quantum plasmonic circuits, and first studies to apply it in more complicated schemes, e.g. to generate entanglement [216], have been performed.

8.2. Phonons

In addition to photons and plasmons, there are other quasi-particles resulting from a quantum mechanical description of excited modes, e.g. phonons that are the quantized excitation of mechanical motions. Phonons also follow Bose–Einstein statistics, and as such they are expected to bunch in an HOM-like arrangement. Recently, such a two-phonon interference effect has been observed involving two trapped ions [209]. In the experiment, the excitations of the radial modes of the trapped Ca^+ ions served as the phonons. After cooling the ions to the ground state, a two-pulse sequence brought the ions to an excited state followed by a re-initialization back to the ground state leaving phononic excitations at both ions. A subsequent time period with no laser irradiation allowed the phonons to hop to the neighbouring ion. Finally, a read-out pulse filtering states of phonons at two different ions was applied. For waiting times when the hopping probability of the phonons was 50%, bunching was observed (see figures 8(c) and (d)). Although the statistical significance of the fidelity was too small to exclude classical explanations with certainty (0.52 ± 0.03), the experiment opens the path to phonon quantum information experiments, such as boson sampling or entanglement generation in larger ion crystals, relying on a phononic HOM interference. A nice example recently demonstrated a quantum walk with phonons implemented in a trapped ion crystal [217].

8.3. Collective atomic excitations

In the previous paragraph, excitations of atoms were used to generate phonons in an ion crystal in a controlled manner. However, collective excitations have also been tested with

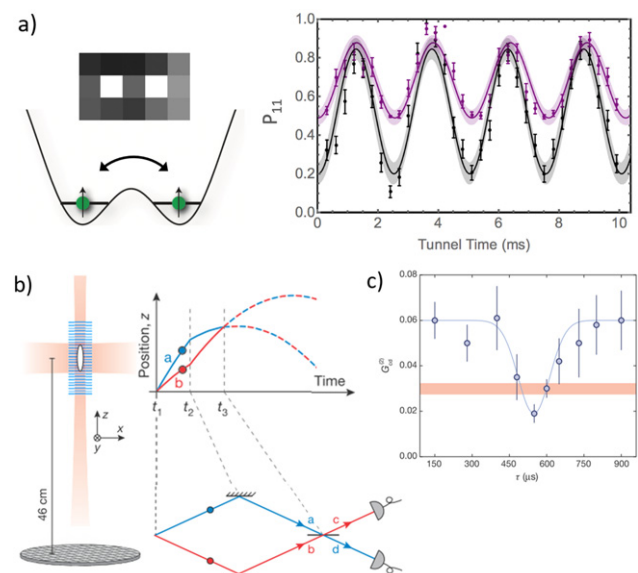


Figure 9. Atomic HOM interference. (a) Two single atoms were trapped in an optical tweezer and made indistinguishable by ground state cooling. Inset shows a camera picture of the atoms. Coupling between the trapping potentials allows for a tunnelling probability of 50%. Since the first two cases cancel out each other, the atoms bunch and are always found in one trap (image courtesy of Cindy Regal and Brian Lester). Reproduced with permission from Cindy Regal and Brian Lester. (b) HOM experiment with a twin-pair source of ^4He atoms. The twin-pairs are produced by imprinting optical gratings leading to a four-wave mixing process, beam reflection and splitting. With the help of multichannel detectors, spatio-temporal imaging and momentum distribution measurements were performed. (c) Measured cross-correlation between atoms found in different output ports depending on the time between mirror and beam splitter, i.e. their distinguishability (b), (c) Reprinted by permission from Springer Nature Customer Service Centre GmbH: Nature. [217] © 2015.

respect to interference effects in a recent experiment using a Rb ensemble [210]. By using the Rydberg blockade, two distinct collective excitations in different Zeeman levels have been generated. Using a stimulating Raman pulse that acts as a beam splitter, the excitations can be interfered and bunched together in either of the two Zeeman states (see figure 8(e)). A final Raman readout pulse leads to an emission of the two photons. Similar to photonic experiments, bunching was confirmed through a dip with a visibility up to 0.89 ± 0.06 in the correlation measurements of the two photons (see figure 8(f)) by varying the distinguishability and splitting ratio.

8.4. Atoms

So far, we have only discussed quasi-particles, i.e. quantized excitation of photonic, plasmonic or phononic modes. However, following quantum mechanics, even massive particles should be able to exhibit two-particle interferences. In fact, two recent experiments, both using very different approaches, have shown exactly this: a two-atom HOM interference. In one experiment, two laser-cooled Rb atoms trapped in an optical tweezer were perfectly controlled in all internal and external degrees of freedom, thereby making them indistinguishable [218]. By carefully tuning the position and depth of the tweezer

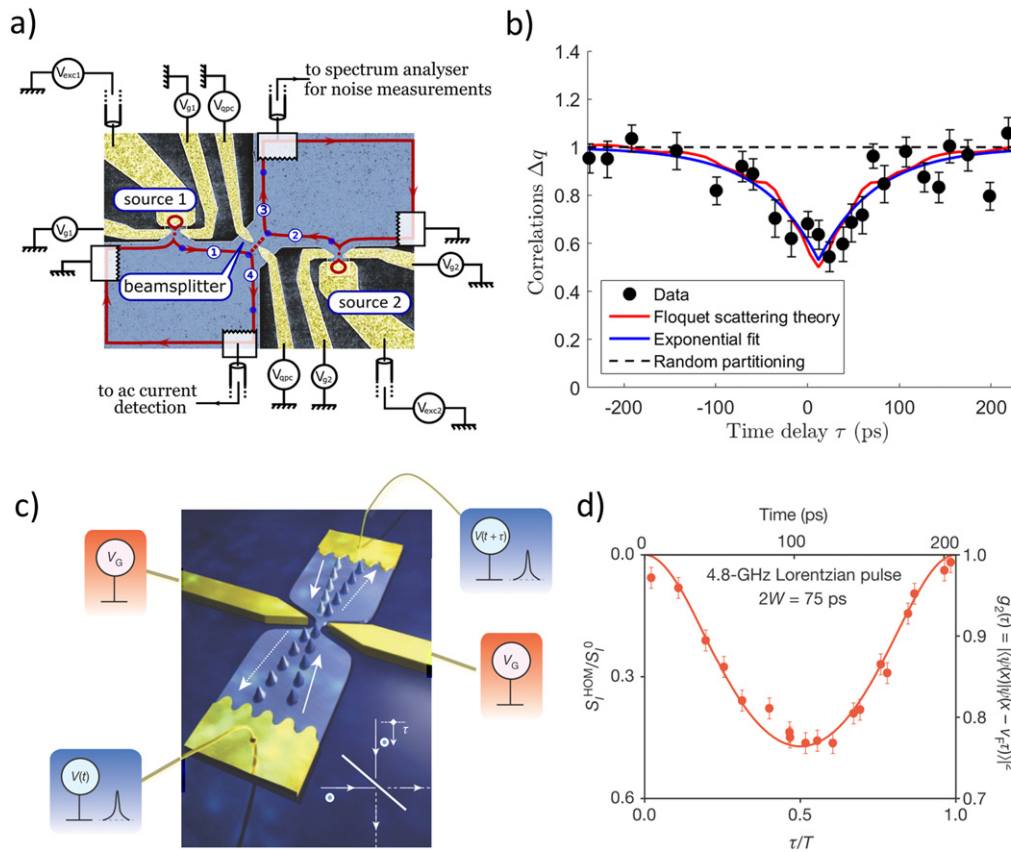


Figure 10. Electronic HOM experiments. (a) Two quantum dots (source 1 and 2) emit single electrons into chiral edges states in a two-dimensional electron gas. A quantum point contact acts as a 50:50 beam splitter. (b) The joint measurement of the noise properties (labelled as correlation Δq) are found to be lower than classically allowed due to anti-bunching of the electrons; thus, a Pauli-dip appears if the delay between the two electrons is zero at the beam splitter (a), (b) Reproduced with permission from Gwendal Feve. (c) Two levitons are emitted into an electronic gas by applying a Lorentzian pulse to two opposing contacts. (d) Again, noise properties corresponding to correlation measurements reveal anti-bunching depending on the delay between the two emissions (c), (d) Reprinted by permission from Springer Nature Customer Service Centre GmbH: Nature. [230] © 2013.

ers, the bosonic atoms were allowed to tunnel between the two traps. After a specific amount of time, a 50% probability of tunnelling of the atoms to the neighbouring trap can be realized (see figure 9(a)). The resulting probability of finding two indistinguishable atoms in one trap exceeded the probability for distinguishable atoms by 6 standard deviations, which can be considered a clear indication for bunching of massive systems. Shortly after this initial step, these results were extended to a complex quantum walk of atoms in a two-dimensional optical lattice [219].

After this HOM experiment with trapped single atoms, another experiment was performed using metastable ^4He atoms released from a Bose–Einstein condensate (BEC) consisting of around 5×10^4 atoms [220]. At first, a moving optical lattice was superimposed on the BEC, which induced a scattering of the atoms along the vertical direction (see figure 9(b)) through a process similar to optical spontaneous four-wave mixing. The scattering led to a beam of twin-atoms at two different velocities that moved apart under the influence of gravity. A few hundred microseconds later, another optical lattice imposed Bragg diffraction on both beams to swap their velocities and bring them back together. Finally, when the two trajectories met again, a last grating imposed a 50:50 BS oper-

ation on the twin atoms and enabled the interference. Using a micro-channel plate to detect the falling atoms, the cross-correlation between the two detected velocities, i.e. the two output channels of the BS, was measured while changing the time of the last grating, i.e. the splitting ratio. Again, the results show a clear dip in the cross-correlation measurements with a visibility of 0.65 ± 0.07 , which is above the classical limit of 0.5 and as such a proof for atomic bunching [221]. While both experiments show impressive results for atomic HOM experiments, future research in this direction could enable multi-particle interferences, entanglement operations and quantum information tasks [222, 223] known from the mature field of quantum optics.

8.5. Electrons

Finally, it has been shown that not only bosons but also fermions in the form of electrons can interfere in an HOM-like arrangement. The major difference between indistinguishable bosons and fermions is that the latter obey Fermi statistics, which leads to anti-bunching at a BS. Fermionic two-particle interferences are a manifestation of the Pauli exclusion-principle. The first such interference was studied in 1998 with a constant stream of colliding electrons pro-

duced in a two-dimensional electron gas [224]. A small gate finger in the centre of the scattering area enabled the tuning of the splitting ratio to around 50% transmission. Due to anti-bunching, a reduction in the noise properties of the output ports was observed; thus, an indirect verification of two-electron anti-bunching was achieved. However, because these initial findings used a continuous stream of electrons, the interference might not exclusively be interpreted as a result from the overlap between two single-electron wave packets. Recently, this deficiency was resolved by an improved experiment, using two separate sources of single electrons emitted from a triggered quantum dot [225, 226]. By applying a voltage pulse to the dot with an energy far above the Fermi level, single electrons are generated followed by the emission of a single hole [227]. The electrons are emitted into chiral edge states and propagate along the edges of a two-dimensional electron gas in the quantum Hall regime. The electronic BS is realized by a narrow constriction, also called quantum point contact. As single coincidence detections are not possible, the correlation noise properties at the outputs were studied and found to be below the random partition noise, i.e. classically expected noise (see figures 10(a) and (b)). If one electron is delayed, the noise properties change such that a Pauli-dip (analog to the HOM-dip for coincidences measurements) of around 50% of the classical noise level was observed.

Following these experiments, the HOM interference was further applied to study an electron gas in the integer quantum Hall regime at a filling factor of 2, where a charge transport along two co-propagating edge channels with opposite spin occurs [228]. Similarly, HOM has also been used to test single electron decoherence in quantum Hall edge channels for excitations emitted at a finite energy above the Fermi sea (by the quantum dot source) [229]. For a comprehensive study on the link between electron quantum optics and quantum signal processing, see [230]. Recently, HOM has been performed in the fractional quantum Hall effect using a device with BSs that are able to scatter fractional statistics excitations (anyons) [231]. This provides the first direct evidence of non-trivial statistics by looking for the signature of anyonic statistics on the current correlations, as predicted in [232].

Interestingly, electronic systems also permit the generation and manipulation of quasi-particles, so-called levitons. A leviton is the quantized minimal excitation of the electronic Fermi sea in a conductor for which no hole is generated. Compared to the electron described above, which can be seen as energy-resolved sources, levitons can be described as a time-resolved excitation. They are triggered by a well-adjusted Lorentzian voltage pulse during which only a positive energy boost is given to the Fermi sea. Although such electronic quasi-particles have been predicted a long time ago [234, 235], they have been observed and even brought to two-fermionic quantum interference only recently [233]. After the emission from two ohmic contacts into a two-dimensional electron gas, levitons propagate through a quantum point contact that acts as a 50:50 BS. From the noise measurements, a $g^{(2)}$ value up to 1 was deduced if both levitons were emitted simultaneously,

which is a signature for anti-bunching. Because levitons are propagating with less disturbance, the visibility of the interference is significantly higher than the one of the electronic HOM interference described in the last paragraph (see figure 10(b)). This feature also led to an intensive study of levitons in the quantum regime [236], for example by investigating the temperature dependence on the indistinguishability [237] or by performing quantum tomography on an electron [238–240].

9. Conclusion

Two-photon interference is fundamentally interesting because it has no classical counterpart, with many applications ranging from precision measurement and state determination to quantum computations and quantum communication. In metrology, two photon interference allows for femtosecond and even attosecond time-resolution, state determination (quantum state analysis), and generating non-classical light for resolution enhancement with linear optics. In quantum state analysis, it gives the possibility to distinguish between modes, since only indistinguishable states will bunch. In particular, two-photon interference enables the measurement of maximally entangled states through Bell state measurements, or equivalently, the projection onto the Bell basis. Indeed, Bell state measurements are central to the concepts of teleportation and entanglement swapping. In quantum communication, it can be used to circumvent the problem of untrusted measurement devices, and build novel protocols. In quantum computation, the interaction between two photons is often required to create the building blocks of certain quantum gates, for example CNOT and CZ gates. Two-photon interference acts as the linear optical solution to this challenge, and thus provides a scalable technique to build photonic quantum computers. Two particle interferences is not only the basis for most of optical quantum information science and a powerful tool for metrology and other fields—its observation being pushed to well beyond the laboratory scale [241]—but it has also led to many fundamental demonstrations in non-photonic systems such as plasmons, phonons, atoms and electrons. Moreover, it still inspires physicists to study its connection to novel systems such as quantized spin waves, i.e. magnons [242], Bogoliubov quasiparticles [243], massless Dirac fermions in topological insulators and graphene [244] or to transfer the idea to analog situations, e.g. with bright solitons [245].

Acknowledgments

E K acknowledges the fruitful conversation with Gerd Leuchs, Miles J Padgett, and Sir Peter Knight. All authors acknowledge Cindy Regal and Brian Lester for providing and giving permission to use the images in figure 9(a)). All authors acknowledge Gwendal Fève for providing and giving permission to use the images in figures 10(a) and (b)). This work was supported by Canada Research Chairs (CRC), Canada First Excellence Research Fund (CFREF), and Ontario's Early Researcher Award (ERA).

ORCID iDs

Robert Fickler  <https://orcid.org/0000-0001-6251-753X>
 Fabio Sciarrino  <https://orcid.org/0000-0003-1715-245X>
 Ebrahim Karimi  <https://orcid.org/0000-0002-8168-7304>

References

- [1] Paneru D, Cohen E, Fickler R, Boyd R W and Karimi E 2020 Entanglement: quantum or classical? *Rep. Prog. Phys.* **83** 064001
- [2] Prasad S, Scully M O and Martienssen W 1987 A quantum description of the beam splitter *Opt. Commun.* **62** 139–45
- [3] Ou Z Y, Hong C K and Mandel L 1987 Relation between input and output states for a beam splitter *Opt. Commun.* **63** 118–22
- [4] Hong C K, Ou Z Y and Mandel L 1987 Measurement of sub-picosecond time intervals between two photons by interference *Phys. Rev. Lett.* **59** 2044–6
- [5] Fearn H and Loudon R 1987 Quantum theory of the lossless beam splitter *Opt. Commun.* **64** 485–90
- [6] Rarity J and Tapster P 1988 Nonclassical effects in parametric *Photons Quantum Fluctuations* **5** 122
- [7] Rarity J G and Tapster P R 1989 Fourth-order interference in parametric downconversion *J. Opt. Soc. Am. B* **6** 1221–6
- [8] Abram I, Raj R K, Oudar J L and Dolique G 1986 Direct observation of the second-order coherence of parametrically generated light *Phys. Rev. Lett.* **57** 2516
- [9] Shih Y H and Alley C O 1988 New type of Einstein–Podolsky–Rosen–Bohm experiment using pairs of light quanta produced by optical parametric down conversion *Phys. Rev. Lett.* **61** 2921
- [10] Hamilton M W 2000 Phase shifts in multilayer dielectric beam splitters *Am. J. Phys.* **68** 186–91
- [11] Paul H 1986 Interference between independent photons *Rev. Mod. Phys.* **58** 209–31
- [12] Ou Z Y, Gage E C, Magill B E and Mandel L 1989 Fourth-order interference technique for determining the coherence time of a light beam *J. Opt. Soc. Am. B* **6** 100–3
- [13] Miyamoto Y, Kuga T, Baba M and Matsuoka M 1993 Measurement of ultrafast optical pulses with two-photon interference *Opt. Lett.* **18** 900–2
- [14] Kim Y S, Slattery O, Kuo P S and Tang X 2014 Two-photon interference with continuous-wave multi-mode coherent light *Opt. Express* **22** 3611–20
- [15] Kim H, Lee S M, Kwon O and Moon H S 2017 Observation of two-photon interference effect with a single non-photon-number resolving detector *Opt. Lett.* **42** 2443–6
- [16] Moschandreou E, Garcia J I, Rollick B J, Qi B, Pooser R and Siopsis G 2018 Experimental study of Hong–Ou–Mandel interference using independent phase randomized weak coherent states *J. Lightwave Technol.* **36** 3752–9
- [17] Kim H, Kim D, Park J and Moon H S 2020 Hong–Ou–Mandel interference of two independent continuous-wave coherent photons *Photon. Res.* **8** 1491–5
- [18] Ferreira da Silva T *et al* 2013 Proof-of-principle demonstration of measurement-device-independent quantum key distribution using polarization qubits *Phys. Rev. A* **88** 052303
- [19] Pittman T B, Strekalov D V, Migdall A, Rubin M H, Sergienko A V and Shih Y H 1996 Can two-photon interference be considered the interference of two photons? *Phys. Rev. Lett.* **77** 1917
- [20] Kim Y-H, Chekhova M V, Kulik S P and Shih Y 1999 Quantum interference by two temporally distinguishable pulses *Phys. Rev. A* **60** R37
- [21] Kim D, Park J, Jeong T, Kim H and Moon H S 2020 Two-photon interference between continuous-wave coherent photons temporally separated by a day *Photon. Res.* **8** 338–42
- [22] Einstein A, Podolsky B and Rosen N 1935 Can quantum-mechanical description of physical reality be considered complete? *Phys. Rev.* **47** 777
- [23] Ekert A K 1991 Quantum cryptography based on Bell’s theorem *Phys. Rev. Lett.* **67** 661
- [24] Dowling J P 2008 Quantum optical metrology—the lowdown on high-N00N states *Contemp. Phys.* **49** 125–43
- [25] Kok P, Munro W J, Nemoto K, Ralph T C, Dowling J P and Milburn G J 2007 Linear optical quantum computing with photonic qubits *Rev. Mod. Phys.* **79** 135
- [26] Zeilinger A 1998 Quantum entanglement: a fundamental concept finding its applications *Phys. Scr. T* **76** 203–9
- [27] Nagali E, Sansoni L, Sciarrino F, De Martini F, Marrucci L, Piccirillo B, Karimi E and Santamato E 2009 Optimal quantum cloning of orbital angular momentum photon qubits through Hong–Ou–Mandel coalescence *Nat. Photon.* **3** 720
- [28] Karimi E *et al* 2014 Exploring the quantum nature of the radial degree of freedom of a photon via Hong–Ou–Mandel interference *Phys. Rev. A* **89** 013829
- [29] Slussarenko S, Weston M M, Chrzanowski H M, Shalm L K, Verma V B, Nam S W and Pryde G J 2017 Unconditional violation of the shot-noise limit in photonic quantum metrology *Nat. Photon.* **11** 700–3
- [30] D’Ambrosio V *et al* 2019 Tunable two-photon quantum interference of structured light *Phys. Rev. Lett.* **122** 013601
- [31] Hiekkamäki M and Fickler R 2020 Single-path two-photon interference effects between spatial modes (arXiv:2006.13288)
- [32] Mohanty A *et al* 2017 Quantum interference between transverse spatial waveguide modes *Nat. Commun.* **8** 14010
- [33] Raymer M G, van Enk S J, McKinstrie C J and McGuinness H J 2010 Interference of two photons of different color *Opt. Commun.* **283** 747–52
- [34] Kobayashi T, Ikuta R, Yasui S, Miki S, Yamashita T, Terai H, Yamamoto T, Koashi M and Imoto N 2016 Frequency-domain Hong–Ou–Mandel interference *Nat. Photon.* **10** 441–4
- [35] Rubinsztein-Dunlop H *et al* 2016 Roadmap on structured light *J. Opt.* **19** 013001
- [36] Giovannini D, Romero J, Poto ek V, Ferenczi G, Speirits F, Barnett S M, Faccio D and Padgett M J 2015 Spatially structured photons that travel in free space slower than the speed of light *Science* **347** 857–60
- [37] Bouchard F, Harris J, Mand H, Boyd R W and Karimi E 2016 Observation of subluminal twisted light in vacuum *Optica* **3** 351–4
- [38] Lyons A, Roger T, Westerberg N, Vezzoli S, Maitland C, Leach J, Padgett M J and Faccio D 2018 How fast is a twisted photon? *Optica* **5** 682–6
- [39] Richard G *et al* 2020 Twisting waves increase the visibility of nonlinear behaviour *New J. Phys.* **22** 063021
- [40] Kim H *et al* 2016 Two-photon interference of temporally separated photons *Sci. Rep.* **6** 34805
- [41] Yang Y *et al* 2019 Two-parameter Hong–Ou–Mandel dip *Sci. Rep.* **9** 10821
- [42] Kim H, Lee S M, Kwon O and Moon H S 2017 Two-photon interference of polarization-entangled photons in a Franson interferometer *Sci. Rep.* **7** 5772
- [43] Lyons A, Knee G C, Bolduc E, Roger T, Leach J, Gauger E M and Faccio D 2018 Attosecond-resolution Hong–Ou–Mandel interferometry *Sci. Adv.* **4** eaap9416
- [44] Chen Y, Fink M, Steinlechner F, Torres J P and Ursin R 2019 Hong–Ou–Mandel interferometry on a biphoton beat note *npj Quantum Inf.* **5** 1–6

- [45] Scott H, Branford D, Westerberg N, Leach J and Gauger E M 2020 Beyond coincidence in Hong–Ou–Mandel interferometry *Phys. Rev. A* **102** 033714
- [46] Steinberg A M, Kwiat P G and Chiao R Y 1992 Dispersion cancellation and high-resolution time measurements in a fourth-order optical interferometer *Phys. Rev. A* **45** 6659
- [47] Povazay B *et al* 2002 Submicrometer axial resolution optical coherence tomography *Opt. Lett.* **27** 1800–2
- [48] Abouraddy A F, Nasr M B, Saleh B E, Sergienko A V and Teich M C 2002 Quantum-optical coherence tomography with dispersion cancellation *Phys. Rev. A* **65** 053817
- [49] Nasr M B, Saleh B E, Sergienko A V and Teich M C 2003 Demonstration of dispersion-cancelled quantum-optical coherence tomography *Phys. Rev. Lett.* **91** 083601
- [50] Nasr M B, Saleh B E A, Sergienko A V and Teich M 2004 Dispersion-cancelled and dispersion-sensitive quantum optical coherence tomography *Opt. Express* **12** 1353–62
- [51] Nasr M B, Goode D P, Nguyen N, Rong G, Yang L, Reinhard B M, Saleh B E A and Teich M C 2009 Quantum optical coherence tomography of a biological sample *Opt. Commun.* **282** 1154–9
- [52] Lopez-Mago D and Novotny L 2012 Quantum-optical coherence tomography with collinear entangled photons *Opt. Lett.* **37** 4077–9
- [53] Erkmen B I and Shapiro J H 2006 Phase-conjugate optical coherence tomography *Phys. Rev. A* **74** 041601
- [54] Banaszek K, Radunsky A S and Walmsley I A 2007 Blind dispersion compensation for optical coherence tomography *Opt. Commun.* **269** 152–5
- [55] Resch K J, Puvanathan P, Lundeen J S, Mitchell M W and Bizheva K 2007 Classical dispersion-cancellation interferometry *Opt. Express* **15** 8797–804
- [56] Mazurek M, Schreier K, Prevedel R, Kaltenbaek R and Resch K 2013 Dispersion-cancelled biological imaging with quantum-inspired interferometry *Sci. Rep.* **3** 1582
- [57] Nasr M B, Goode D P, Nguyen N, Rong G, Yang L, Reinhard B M, Saleh B E A and Teich M C 2009 Quantum optical coherence tomography of a biological sample *Opt. Commun.* **282** 1154–9
- [58] Boto A N, Kok P, Abrams D S, Braunstein S L, Williams C P and Dowling J P 2000 Quantum interferometric optical lithography: exploiting entanglement to beat the diffraction limit *Phys. Rev. Lett.* **85** 2733–6
- [59] Giovannetti V, Lloyd S and Maccone L 2011 Advances in quantum metrology *Nat. Photon.* **5** 222
- [60] Rarity J, Tapster P, Jakeman E, Larchuk T, Campos R, Teich M and Saleh B 1990 Two-photon interference in a Mach–Zehnder interferometer *Phys. Rev. Lett.* **65** 1348
- [61] Edamatsu K, Shimizu R and Itoh T 2002 Measurement of the photonic de Broglie wavelength of entangled photon pairs generated by spontaneous parametric down-conversion *Phys. Rev. Lett.* **89** 213601
- [62] McCusker K T and Kwiat P G 2009 Efficient optical quantum state engineering *Phys. Rev. Lett.* **103** 163602
- [63] Kapale K T and Dowling J P 2007 Bootstrapping approach for generating maximally path-entangled photon states *Phys. Rev. Lett.* **99** 053602
- [64] Cable H and Dowling J P 2007 Efficient generation of large number-path entanglement using only linear optics and feed-forward *Phys. Rev. Lett.* **99** 163604
- [65] Pezzé L and Smerzi A 2008 Mach–Zehnder interferometry at the Heisenberg limit with coherent and squeezed-vacuum light *Phys. Rev. Lett.* **100** 073601
- [66] D’Angelo M, Chekhova M V and Shih Y 2001 Two-photon diffraction and quantum lithography *Phys. Rev. Lett.* **87** 013602
- [67] Mitchell M W, Lundeen J S and Steinberg A M 2004 Super-resolving phase measurements with a multiphoton entangled state *Nature* **429** 161
- [68] Walther P, Pan J-W, Aspelmeyer M, Ursin R, Gasparoni S and Zeilinger A 2004 De Broglie wavelength of a non-local four-photon state *Nature* **429** 158
- [69] Kim H, Park H S and Choi S-K 2009 Three-photon N00N states generated by photon subtraction from double photon pairs *Opt. Express* **17** 19720–6
- [70] Liu B *et al* 2008 Demonstration of the three-photon de Broglie wavelength by projection measurement *Phys. Rev. A* **77** 023815
- [71] Resch K J *et al* 2007 Time-reversal and super-resolving phase measurements *Phys. Rev. Lett.* **98** 223601
- [72] Okamoto R, Hofmann H F, Nagata T, O’Brien J L, Sasaki K and Takeuchi S 2008 Beating the standard quantum limit: phase super-sensitivity of N-photon interferometers *New J. Phys.* **10** 073033
- [73] Nagata T, Okamoto R, O’Brien J L, Sasaki K and Takeuchi S 2007 Beating the standard quantum limit with four-entangled photons *Science* **316** 726–9
- [74] Afek I, Ambar O and Silberberg Y 2010 High-N00N states by mixing quantum and classical light *Science* **328** 879–81
- [75] Zhou Z-Y *et al* 2017 Superresolving phase measurement with short-wavelength noon states by quantum frequency up-conversion *Phys. Rev. Appl.* **7** 064025
- [76] Kaltenbaek R, Blauensteiner B, Żukowski M, Aspelmeyer M and Zeilinger A 2006 Experimental interference of independent photons *Phys. Rev. Lett.* **96** 240502
- [77] Mosley P J *et al* 2008 Heralded generation of ultrafast single photons in pure quantum states *Phys. Rev. Lett.* **100** 133601
- [78] Sanaka K, Pawlis A, Ladd T D, Lischka K and Yamamoto Y 2009 Indistinguishable photons from independent semiconductor nanostructures *Phys. Rev. Lett.* **103** 053601
- [79] Flagg E B *et al* 2010 Interference of single photons from two separate semiconductor quantum dots *Phys. Rev. Lett.* **104** 137401
- [80] Patel R B, Bennett A J, Farrer I, Nicoll C A, Ritchie D A and Shields A J 2010 Two-photon interference of the emission from electrically tunable remote quantum dots *Nat. Photon.* **4** 632
- [81] Wei Y-J *et al* 2014 Deterministic and robust generation of single photons from a single quantum dot with 99.5% indistinguishability using adiabatic rapid passage *Nano Lett.* **14** 6515–9
- [82] Senellart P, Solomon G and White A 2017 High-performance semiconductor quantum-dot single-photon sources *Nat. Nanotechnol.* **12** 1026–39
- [83] Felinto D, Chou C W, Laurat J, Schomburg E W, de Riedmatten H and Kimble H J 2006 Conditional control of the quantum states of remote atomic memories for quantum networking *Nat. Phys.* **2** 844
- [84] Chaneliere T *et al* 2007 Quantum interference of electromagnetic fields from remote quantum memories *Phys. Rev. Lett.* **98** 113602
- [85] Yuan Z-S *et al* 2007 Synchronized independent narrow-band single photons and efficient generation of photonic entanglement *Phys. Rev. Lett.* **98** 180503
- [86] Yuan Z-S, Chen Y-A, Zhao B, Chen S, Schmiedmayer J and Pan J-W 2008 Experimental demonstration of a bdcz quantum repeater node *Nature* **454** 1098
- [87] Chen Y-A, Chen S, Yuan Z-S, Zhao B, Chu C-S, Schmiedmayer J and Pan J-W 2008 Memory-built-in quantum teleportation with photonic and atomic qubits *Nat. Phys.* **4** 103
- [88] Bernien H *et al* 2012 Two-photon quantum interference from separate nitrogen vacancy centers in diamond *Phys. Rev. Lett.* **108** 043604

- [89] Sipahigil A *et al* 2012 Quantum interference of single photons from remote nitrogen-vacancy centers in diamond *Phys. Rev. Lett.* **108** 143601
- [90] Sipahigil A *et al* 2014 Indistinguishable photons from separated silicon-vacancy centers in diamond *Phys. Rev. Lett.* **113** 113602
- [91] Maunz P, Moehring D L, Olmschenk S, Younge K C, Matsukevich D N and Monroe C 2007 Quantum interference of photon pairs from two remote trapped atomic ions *Nat. Phys.* **3** 538
- [92] Beugnon J, Jones M P A, Dingjan J, Darquié B, Messin G, Browaeys A and Grangier P 2006 Quantum interference between two single photons emitted by independently trapped atoms *Nature* **440** 779
- [93] Specht H P, Nölleke C, Reiserer A, Uphoff M, Figueroa E, Ritter S and Rempe G 2011 A single-atom quantum memory *Nature* **473** 190
- [94] Kiraz A *et al* 2005 Indistinguishable photons from a single molecule *Phys. Rev. Lett.* **94** 223602
- [95] Lettow R *et al* 2010 Quantum interference of tunably indistinguishable photons from remote organic molecules *Phys. Rev. Lett.* **104** 123605
- [96] Calsamiglia J and Lütkenhaus N 2001 Maximum efficiency of a linear-optical Bell-state analyzer *Appl. Phys. B* **72** 67–71
- [97] Kim Y-H, Kulik S P and Shih Y 2001 Quantum teleportation of a polarization state with a complete bell state measurement *Phys. Rev. Lett.* **86** 1370
- [98] Kwiat P G and Weinfurter H 1998 Embedded bell-state analysis *Phys. Rev. A* **58** R2623
- [99] Barreiro J T, Wei T-C and Kwiat P G 2008 Beating the channel capacity limit for linear photonic superdense coding *Nat. Phys.* **4** 282
- [100] Knill E, Laflamme R and Milburn G J 2001 A scheme for efficient quantum computation with linear optics *Nature* **409** 46
- [101] Grice W P 2011 Arbitrarily complete bell-state measurement using only linear optical elements *Phys. Rev. A* **84** 042331
- [102] Gisin N, Ribordy G, Tittel W and Zbinden H 2002 Quantum cryptography *Rev. Mod. Phys.* **74** 145
- [103] Pirandola S *et al* 2019 Advances in quantum cryptography (arXiv:1906.01645)
- [104] Wootters W K and Zurek W H 1982 A single quantum cannot be cloned *Nature* **299** 802–3
- [105] Shor P W and Preskill J 2000 Simple proof of security of the bb84 quantum key distribution protocol *Phys. Rev. Lett.* **85** 441
- [106] Zukowski M, Zeilinger A, Horne M A and Ekert A K 1993 ‘Event-ready-detectors’ Bell experiment via entanglement swapping *Phys. Rev. Lett.* **71** 4287–90
- [107] Bennett C H, Brassard G, Crépeau C, Jozsa R, Peres A and Wootters W K 1993 Teleporting an unknown quantum state via dual classical and Einstein–Podolsky–Rosen channels *Phys. Rev. Lett.* **70** 1895
- [108] Bennett C H and Wiesner S J 1992 Communication via one- and two-particle operators on Einstein–Podolsky–Rosen states *Phys. Rev. Lett.* **69** 2881
- [109] Braunstein S L and Pirandola S 2012 Side-channel-free quantum key distribution *Phys. Rev. Lett.* **108** 130502
- [110] Lo H-K, Curty M and Qi B 2012 Measurement-device-independent quantum key distribution *Phys. Rev. Lett.* **108** 130503
- [111] Guan J-Y *et al* 2015 Experimental passive round-robin differential phase-shift quantum key distribution *Phys. Rev. Lett.* **114** 180502
- [112] Hofmann J, Krug M, Ortegell N, Gérard L, Weber M, Rosenfeld W and Weinfurter H 2012 Heralded entanglement between widely separated atoms *Science* **337** 72–5
- [113] Bell J S 1964 On the Einstein–Podolsky–Rosen paradox *Physics* **1** 195–200
- [114] Narla A *et al* 2016 Robust concurrent remote entanglement between two superconducting qubits *Phys. Rev. X* **6** 031036
- [115] Sangouard N, Simon C, De Riedmatten H and Gisin N 2011 Quantum repeaters based on atomic ensembles and linear optics *Rev. Mod. Phys.* **83** 33
- [116] Briegel H-J, Dür W, Cirac J I and Zoller P 1998 Quantum repeaters: the role of imperfect local operations in quantum communication *Phys. Rev. Lett.* **81** 5932
- [117] Fung C-H F, Qi B, Tamaki K and Lo H-K 2007 Phase-remapping attack in practical quantum-key-distribution systems *Phys. Rev. A* **75** 032314
- [118] Zhao Y, Fung C-H F, Qi B, Chen C and Lo H-K 2008 Quantum hacking: experimental demonstration of time-shift attack against practical quantum-key-distribution systems *Phys. Rev. A* **78** 042333
- [119] Lydersen L, Wiechers C, Wittmann C, Elser D, Skaar J and Makarov V 2010 Hacking commercial quantum cryptography systems by tailored bright illumination *Nat. Photon.* **4** 686
- [120] Gerhardt I *et al* 2011 Full-field implementation of a perfect eavesdropper on a quantum cryptography system *Nat. Commun.* **2** 349
- [121] Mayers D and Yao A 1998 *Proc. 39th Annual Symp. Foundations of Computer Science (focs98)*
- [122] Acín A *et al* 2007 Device-independent security of quantum cryptography against collective attacks *Phys. Rev. Lett.* **98** 230501
- [123] Liu Y *et al* 2013 Experimental measurement-device-independent quantum key distribution *Phys. Rev. Lett.* **111** 130502
- [124] Tang Z *et al* 2014 Experimental demonstration of polarization encoding measurement-device-independent quantum key distribution *Phys. Rev. Lett.* **112** 190503
- [125] Tang Y-L *et al* 2014 Measurement-device-independent quantum key distribution over 200 km *Phys. Rev. Lett.* **113** 190501
- [126] Yin H-L *et al* 2016 Measurement-device-independent quantum key distribution over a 404 km optical fiber *Phys. Rev. Lett.* **117** 190501
- [127] Lo H-K, Ma X and Chen K 2005 Decoy state quantum key distribution *Phys. Rev. Lett.* **94** 230504
- [128] Pirandola S, Ottaviani C, Spedalieri G, Weedbrook C, Braunstein S L, Lloyd S, Gehring T, Jacobsen C S and Andersen U L 2015 High-rate measurement-device-independent quantum cryptography *Nat. Photon.* **9** 397–402
- [129] Sasaki T, Yamamoto Y and Koashi M 2014 Practical quantum key distribution protocol without monitoring signal disturbance *Nature* **509** 475
- [130] Takesue H, Sasaki T, Tamaki K and Koashi M 2015 Experimental quantum key distribution without monitoring signal disturbance *Nat. Photon.* **9** 827
- [131] Wang S *et al* 2015 Experimental demonstration of a quantum key distribution without signal disturbance monitoring *Nat. Photon.* **9** 832
- [132] Li Y-H *et al* 2016 Experimental round-robin differential phase-shift quantum key distribution *Phys. Rev. A* **93** 030302
- [133] Yin Z-Q *et al* 2018 Improved security bound for the round-robin-differential-phase-shift quantum key distribution *Nat. Commun.* **9** 457
- [134] Bouchard F, Sit A, Heshami K, Fickler R and Karimi E 2018 Round-robin differential-phase-shift quantum key distribution with twisted photons *Phys. Rev. A* **98** 010301
- [135] Islam N T, Lim C C W, Cahall C, Qi B, Kim J and Gauthier D J 2019 Scalable high-rate, high-dimensional time-bin encoding quantum key distribution *Quantum Sci. Technol.* **4** 035008
- [136] Choi M-D 1975 Completely positive linear maps on complex matrices *Linear Algebra Appl.* **10** 285–90

- [137] Jamiolkowski A 1972 Linear transformations which preserve trace and positive semidefiniteness of operators *Rep. Math. Phys.* **3** 275–8
- [138] Zhang Y, Roux F S, Konrad T, Agnew M, Leach J and Forbes A 2016 Engineering two-photon high-dimensional states through quantum interference *Sci. Adv.* **2** e1501165
- [139] Zhao T-M *et al* 2014 Entangling different-color photons via time-resolved measurement and active feed forward *Phys. Rev. Lett.* **112** 103602
- [140] Peres A 2003 How the no-cloning theorem got its name *Fortschr. Phys.* **51** 458–61
- [141] Navez P and Cerf N J 2003 Cloning a real d-dimensional quantum state on the edge of the no-signaling condition *Phys. Rev. A* **68** 032313
- [142] Nagali E *et al* 2010 Experimental optimal cloning of four-dimensional quantum states of photons *Phys. Rev. Lett.* **105** 073602
- [143] Bouchard F, Fickler R, Boyd R W and Karimi E 2017 High-dimensional quantum cloning and applications to quantum hacking *Sci. Adv.* **3** e1601915
- [144] De Martini F, Bužek V, Sciarrino F and Sias C 2002 Experimental realization of the quantum universal not gate *Nature* **419** 815–8
- [145] Ricci M, Sciarrino F, Sias C and De Martini F 2004 Teleportation scheme implementing the universal optical quantum cloning machine and the universal not gate *Phys. Rev. Lett.* **92** 047901
- [146] Vitelli C, Spagnolo N, Aparo L, Sciarrino F, Santamato E and Marrucci L 2013 Joining the quantum state of two photons into one *Nat. Photon.* **7** 521
- [147] Passaro E *et al* 2013 Joining and splitting the quantum states of photons *Phys. Rev. A* **88** 062321
- [148] Knill E 2003 Bounds on the probability of success of postselected nonlinear sign shifts implemented with linear optics *Phys. Rev. A* **68** 064303
- [149] Ralph T, White A, Munro W and Milburn G 2001 Simple scheme for efficient linear optics quantum gates *Phys. Rev. A* **65** 012314
- [150] Zou X, Pahlke K and Mathis W 2002 Teleportation implementation of nondeterministic quantum logic operations by using linear optical elements *Phys. Rev. A* **65** 064305
- [151] Scheel S, Pachos J, Hinds E and Knight P 2004 Quantum gates and decoherence (arXiv:quant-ph/0403152)
- [152] Knill E 2002 Quantum gates using linear optics and postselection *Phys. Rev. A* **66** 052306
- [153] Okamoto R, O’Brien J L, Hofmann H F and Takeuchi S 2011 Realization of a Knill–Laflamme–Milburn controlled-not photonic quantum circuit combining effective optical nonlinearities *Proc. Natl Acad. Sci.* **108** 10067–71
- [154] Harrow A W, Hassidim A and Lloyd S 2009 Quantum algorithm for linear systems of equations *Phys. Rev. Lett.* **103** 150502
- [155] Cai X-D *et al* 2013 Experimental quantum computing to solve systems of linear equations *Phys. Rev. Lett.* **110** 230501
- [156] Fisher K *et al* 2014 Quantum computing on encrypted data *Nat. Commun.* **5** 3074
- [157] Weimann S *et al* 2016 Implementation of quantum and classical discrete fractional fourier transforms *Nat. Commun.* **7** 11027
- [158] Humphreys P C *et al* 2013 Linear optical quantum computing in a single spatial mode *Phys. Rev. Lett.* **111** 150501
- [159] O’Brien J L, Furusawa A and Vučković J 2009 Photonic quantum technologies *Nat. Photon.* **3** 687
- [160] Wang J, Sciarrino F, Laing A and Thompson M G 2020 Integrated photonic quantum technologies *Nat. Photon.* **14** 273–84
- [161] Garcia-Escartin J C and Chamorro-Posada P 2013 Swap test and Hong–Ou–Mandel effect are equivalent *Phys. Rev. A* **87** 052330
- [162] Zeilinger A, Zukowski M, Horne M, Bernstein H and Greenberger D 1993 Einstein–Podolsky–Rosen correlations in higher dimensions *Fundamental Aspects of Quantum Theory* (Singapore: World Scientific)
- [163] Reck M, Zeilinger A, Bernstein H J and Bertani P 1994 Experimental realization of any discrete unitary operator *Phys. Rev. Lett.* **73** 58
- [164] Weihs G, Reck M, Weinfurter H and Zeilinger A 1996 Two-photon interference in optical fiber multiports *Phys. Rev. A* **54** 893
- [165] Ou Z Y 2007 *Multi-Photon Quantum Interference* (Berlin: Springer)
- [166] Żukowski M, Zeilinger A and Horne M A 1997 Realizable higher-dimensional two-particle entanglements via multiport beam splitters *Phys. Rev. A* **55** 2564
- [167] Campos R A 2000 Three-photon Hong–Ou–Mandel interference at a multiport mixer *Phys. Rev. A* **62** 013809
- [168] Spagnolo N *et al* 2013 Three-photon bosonic coalescence in an integrated tritter *Nat. Commun.* **4** 1606
- [169] Schaeff C, Polster R, Huber M, Ramelow S and Zeilinger A 2015 Experimental access to higher-dimensional entangled quantum systems using integrated optics *Optica* **2** 523–9
- [170] Meany T, Delanty M, Gross S, Marshall G D, Steel M J and Withford M J 2012 Non-classical interference in integrated 3D multiports *Opt. Express* **20** 26895–905
- [171] Menssen A J *et al* 2017 Distinguishability and many-particle interference *Phys. Rev. Lett.* **118** 153603
- [172] Spagnolo N *et al* 2012 Quantum interferometry with three-dimensional geometry *Sci. Rep.* **2** 862
- [173] Tichy M C 2014 Interference of identical particles from entanglement to boson-sampling *J. Phys. B: At. Mol. Opt. Phys.* **47** 103001
- [174] de Guise H, Tan S-H, Poulin I P and Sanders B C 2014 Coincidence landscapes for three-channel linear optical networks *Phys. Rev. A* **89** 063819
- [175] Shchesnovich V 2015 Partial indistinguishability theory for multiphoton experiments in multiport devices *Phys. Rev. A* **91** 013844
- [176] Tichy M C, Tiersch M, de Melo F, Mintert F and Buchleitner A 2010 Zero-transmission law for multiport beam splitters *Phys. Rev. Lett.* **104** 220405
- [177] Tichy M C *et al* 2011 Four-photon indistinguishability transition *Phys. Rev. A* **83** 062111
- [178] Tichy M C, Tiersch M, Mintert F and Buchleitner A 2012 Many-particle interference beyond many-boson and many-fermion statistics *New J. Phys.* **14** 093015
- [179] Ra Y-S, Tichy M C, Lim H-T, Kwon O, Mintert F, Buchleitner A and Kim Y-H 2013 Nonmonotonic quantum-to-classical transition in multiparticle interference *Proc. Natl Acad. Sci. USA* **110** 1227–31
- [180] Lahini Y *et al* 2012 Quantum walk of two interacting bosons *Phys. Rev. A* **86** 011603
- [181] Poem E, Gilead Y and Silberberg Y 2012 Two-photon path-entangled states in multimode waveguides *Phys. Rev. Lett.* **108** 153602
- [182] Defienne H, Barbieri M, Walmsley I A, Smith B J and Gigan S 2016 Two-photon quantum walk in a multimode fiber *Sci. Adv.* **2** e1501054
- [183] Politi A, Matthews J, Thompson M G and O’Brien J L 2009 Integrated quantum photonics *IEEE J. Select. Top. Quantum Electron.* **15** 1673–84
- [184] Peruzzo A *et al* 2010 Quantum walks of correlated photons *Science* **329** 1500–3
- [185] Poullos K *et al* 2014 Quantum walks of correlated photon pairs in two-dimensional waveguide arrays *Phys. Rev. Lett.* **112** 143604
- [186] Owens J O *et al* 2011 Two-photon quantum walks in an elliptical direct-write waveguide array *New J. Phys.* **13** 075003

- [187] Crespi A, Osellame R, Ramponi R, Giovannetti V, Fazio R, Sansoni L, De Nicola F, Sciarrino F and Mataloni P 2013 Anderson localization of entangled photons in an integrated quantum walk *Nat. Photon.* **7** 322
- [188] Sansoni L *et al* 2012 Two-particle Bosonic–Fermionic quantum walk via integrated photonics *Phys. Rev. Lett.* **108** 010502
- [189] Tillmann M *et al* 2015 Generalized multiphoton quantum interference *Phys. Rev. X* **5** 041015
- [190] Metcalf B J *et al* 2013 Multiphoton quantum interference in a multiport integrated photonic device *Nat. Commun.* **4** 1356
- [191] Ferreri A, Ansari V, Silberhorn C and Sharapova P R 2019 Temporally multimode four-photon Hong–Ou–Mandel interference *Phys. Rev. A* **100** 053829
- [192] Luo Y-H *et al* 2019 Quantum teleportation in high dimensions *Phys. Rev. Lett.* **123** 070505
- [193] Tichy M C, Mintert F and Buchleitner A 2013 Limits to multipartite entanglement generation with bosons and fermions *Phys. Rev. A* **87** 022319
- [194] Aaronson S and Arkhipov A 2011 The computational complexity of linear optics *Proc. Forty-Third Annual ACM Symp. Theory of Computing* vol 333–342 (New York: ACM)
- [195] Brod D *et al* 2019 Photonic implementation of boson sampling: a review *Adv. Photon.* **1** 034001
- [196] Broome M A, Fedrizzi A, Rahimi-Keshari S, Dove J, Aaronson S, Ralph T C and White A G 2013 Photonic boson sampling in a tunable circuit *Science* **339** 794–8
- [197] Spring J B *et al* 2012 Boson sampling on a photonic chip *Science* **339** 798–801
- [198] Tillmann M, Dakić B, Heilmann R, Nolte S, Szameit A and Walther P 2013 Experimental boson sampling *Nat. Photon.* **7** 540
- [199] Crespi A *et al* 2013 Integrated multimode interferometers with arbitrary designs for photonic boson sampling *Nat. Photon.* **7** 545
- [200] Spagnolo N *et al* 2014 Experimental validation of photonic boson sampling *Nat. Photon.* **8** 615
- [201] Bentivegna M *et al* 2015 Experimental scattershot boson sampling *Sci. Adv.* **1** e1400255
- [202] Lund A *et al* 2014 Boson sampling from a Gaussian state *Phys. Rev. Lett.* **113** 100502
- [203] Wang H *et al* 2017 High-efficiency multiphoton boson sampling *Nat. Photon.* **11** 361
- [204] Tame M S, McEnery K R, Özdemir Ş K, Lee J, Maier S A and Kim M S 2013 Quantum plasmonics *Nat. Phys.* **9** 329
- [205] Marquier F, Sauvan C and Greffet J-J 2017 Revisiting quantum optics with surface plasmons and plasmonic resonators *ACS Photon.* **4** 2091–101
- [206] Fujii G, Segawa T, Mori S, Namekata N, Fukuda D and Inoue S 2012 Preservation of photon indistinguishability after transmission through surface-plasmon-polariton waveguide *Opt. Lett.* **37** 1535–7
- [207] Wang S M, Mu S Y, Zhu C, Gong Y X, Xu P, Liu H, Li T, Zhu S N and Zhang X 2012 Hong–Ou–Mandel interference mediated by the magnetic plasmon waves in a three-dimensional optical metamaterial *Opt. Express* **20** 5213–8
- [208] Heeres R W, Kouwenhoven L P and Zwiller V 2013 Quantum interference in plasmonic circuits *Nat. Nanotechnol.* **8** 719
- [209] Toyoda K, Hiji R, Noguchi A and Urabe S 2015 Hong–Ou–Mandel interference of two phonons in trapped ions *Nature* **527** 74
- [210] Li J *et al* 2016 Hong–Ou–Mandel interference between two deterministic collective excitations in an atomic ensemble *Phys. Rev. Lett.* **117** 180501
- [211] Fakonas J S, Lee H, Kelaita Y A and Atwater H A 2014 Two-plasmon quantum interference *Nat. Photon.* **8** 317
- [212] Di Martino G *et al* 2014 Observation of quantum interference in the plasmonic Hong–Ou–Mandel effect *Phys. Rev. Appl.* **1** 034004
- [213] Cai Y-J *et al* 2014 High-visibility on-chip quantum interference of single surface plasmons *Phys. Rev. Appl.* **2** 014004
- [214] Fujii G, Fukuda D and Inoue S 2014 Direct observation of bosonic quantum interference of surface plasmon polaritons using photon-number-resolving detectors *Phys. Rev. B* **90** 085430
- [215] Vest B, Dheur M-C, Devaux É, Baron A, Rousseau E, Hugonin J-P, Greffet J-J, Messin G and Marquier F 2017 Anticoalescence of bosons on a lossy beam splitter *Science* **356** 1373–6
- [216] Dieleman F, Tame M S, Sonnefraud Y, Kim M S and Maier S A 2017 Experimental verification of entanglement generated in a plasmonic system *Nano Lett.* **17** 7455–61
- [217] Tamura M, Mukaiyama T and Toyoda K 2020 Quantum walks of a phonon in trapped ions *Phys. Rev. Lett.* **124** 200501
- [218] Kaufman A M, Lester B J, Reynolds C M, Wall M L, Foss-Feig M, Hazzard K R A, Rey A M and Regal C A 2014 Two-particle quantum interference in tunnel-coupled optical tweezers *Science* **345** 306–9
- [219] Preiss P M, Ma R, Tai M E, Lukin A, Rispoli M, Zupancic P, Lahini Y, Islam R and Greiner M 2015 Strongly correlated quantum walks in optical lattices *Science* **347** 1229–33
- [220] Lopes R, Imanaliev A, Aspect A, Cheneau M, Boiron D and Westbrook C I 2015 Atomic Hong–Ou–Mandel experiment *Nature* **520** 66
- [221] Lewis-Swan R and Kheruntsyan K 2014 Proposal for demonstrating the Hong–Ou–Mandel effect with matter waves *Nat. Commun.* **5** 3752
- [222] Dussarrat P *et al* 2017 Two-particle four-mode interferometer for atoms *Phys. Rev. Lett.* **119** 173202
- [223] Kaufman A M, Tichy M C, Mintert F, Rey A M and Regal C A 2018 The Hong–Ou–Mandel effect with atoms *Advances in Atomic, Molecular, and Optical Physics* vol 67 (Amsterdam: Elsevier) pp 377–427
- [224] Liu R C, Odom B, Yamamoto Y and Tarucha S 1998 Quantum interference in electron collision *Nature* **391** 263
- [225] Bocquillon E *et al* 2012 Electron quantum optics: partitioning electrons one by one *Phys. Rev. Lett.* **108** 196803
- [226] Bocquillon E *et al* 2013 Coherence and indistinguishability of single electrons emitted by independent sources *Science* **339** 1054–57
- [227] Fève G, Mahe A, Berroir J-M, Kontos T, Placais B, Glattli D C, Cavanna A, Etienne B and Jin Y 2007 An on-demand coherent single-electron source *Science* **316** 1169–72
- [228] Freulon V *et al* 2015 Hong–Ou–Mandel experiment for temporal investigation of single-electron fractionalization *Nat. Commun.* **6** 6854
- [229] Marguerite A *et al* 2016 Decoherence and relaxation of a single electron in a one-dimensional conductor *Phys. Rev. B* **94** 115311
- [230] Roussel B, Cabart C, Fève G, Thibierge E and Degiovanni P 2017 Electron quantum optics as quantum signal processing *Phys. Status Solidi B* **254** 1600621
- [231] Bartolomei H *et al* 2020 Fractional statistics in anyon collisions *Science* **368** 173–7
- [232] Rosenow B *et al* 2016 Current correlations from a mesoscopic anyon collider *Phys. Rev. Lett.* **116** 156802
- [233] Dubois J, Jullien T, Portier F, Roche P, Cavanna A, Jin Y, Wegscheider W, Roulleau P and Glattli D C 2013 Minimal-excitation states for electron quantum optics using levitons *Nature* **502** 659
- [234] Levitov L S, Lee H and Lesovik G B 1996 Electron counting statistics and coherent states of electric current *J. Math. Phys.* **37** 4845–66
- [235] Keeling J, Klich I and Levitov L 2006 Minimal excitation states of electrons in one-dimensional wires *Phys. Rev. Lett.* **97** 116403
- [236] Glattli D C and Roulleau P S 2017 Levitons for electron quantum optics *Phys. Status Solidi B* **254** 1600650

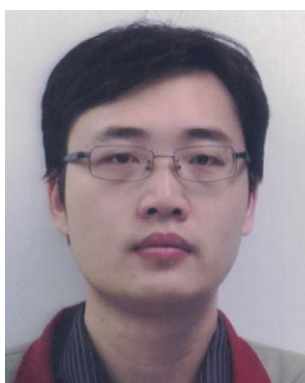
- [237] Glattli D and Roulleau P 2016 Hanbury–Brown twiss noise correlation with time controlled quasi-particles in ballistic quantum conductors *Physica E* **76** 216–22
- [238] Jullien T, Roulleau P, Roche B, Cavanna A, Jin Y and Glattli D C 2014 Quantum tomography of an electron *Nature* **514** 603
- [239] Grenier C *et al* 2011 Single-electron quantum tomography in quantum Hall edge channels *New J. Phys.* **13** 093007
- [240] Bisognin R *et al* 2019 Quantum tomography of electrical currents *Nat. Commun.* **10** 3379
- [241] Deng Y-H *et al* 2019 Quantum interference between light sources separated by 150 million kilometers *Phys. Rev. Lett.* **123** 080401
- [242] Ahmed M H, Jeske J and Greentree A D 2017 Guided magnonic Michelson interferometer *Sci. Rep.* **7** 41472
- [243] Ferraro D, Rech J, Jonckheere T and Martin T 2015 Nonlocal interference and Hong–Ou–Mandel collisions of single bogoliubov quasiparticles *Phys. Rev. B* **91** 075406
- [244] Khan M and Leuenberger M N 2014 Two-dimensional fermionic Hong–Ou–Mandel interference with massless Dirac fermions *Phys. Rev. B* **90** 075439
- [245] Sun Z-Y, Kevrekidis P G and Krüger P 2014 Mean-field analog of the Hong–Ou–Mandel experiment with bright solitons *Phys. Rev. A* **90** 063612



Frédéric Bouchard received his PhD degree in physics from the University of Ottawa, Canada, in 2019. In 2014, he received the University Silver Medal and the Faculty of Science Plaque from the University of Ottawa for his B.Sc. degree for the second-highest standing in the Faculty of Science and for the highest standing in the Department of Physics, respectively. In 2016, he received the Vanier Canada Graduate Scholarship from the National Sciences and Engineering Research Council of Canada for his PhD degree. He has published over 40 scientific articles in peer-reviewed journals. Since 2019, he has been a Research Associate at the National Research Council of Canada working on quantum optics, quantum communication and quantum information.



Alicia Sit received her BSc with a specialization in physics-mathematics and MSc in physics from the University of Ottawa, Canada, in 2017 and 2019, respectively. She is currently pursuing her PhD in physics at the University of Ottawa, exploring the applications of structured light for high-dimensional quantum cryptography in practical free-space quantum channels. She has published over 20 papers. In 2019, she was awarded a Vanier Canada Graduate Scholarship from the Natural Sciences and Engineering Research Council of Canada.



Yingwen Zhang obtained his MSc and PhD at the University of Cape Town in 2013, specializing in High Energy Physics. He later migrated to the field of Quantum Optics and was a post-doctoral fellow at the South Africa Council for Scientific and Industrial Research from 2013-2016 and at the University of Ottawa from 2016-2019. He is currently a research officer at the National Research Council Canada. His current research interest is mainly focused on quantum sensing, more particularly, in quantum imaging and quantum illumination.



Robert Fickler received his masters degree in physics from Ulm University, Germany, in 2009. He also holds a bachelor's degree in philosophy and is a trained electronics engineer. He obtained his PhD degree in 2014 from the University of Vienna, Austria, and worked as a postdoctoral fellow at the University of Ottawa, Canada, and the Institute for Quantum Optics and Quantum Information - Vienna, Austria. Since 2019, he is an Assistant Professor at Tampere University, Finland, where is continuing to work on quantum photonics, quantum information, and light-matter interactions in the quantum regime. He has published more than 50 research papers. His research was named as one of the Top 10 breakthroughs of the year 2012 by IOPs Physics World, he received the Young Scientist Award 2015 of the IUPAP as well as the Banting Postdoctoral Fellowship of the Natural Sciences and Engineering Research Council of Canada 2016.



Yuan Yao is a second-year Ph.D. student in the IQA (Information Quantique et Applications) group at Télécom Paris, and she is working under the supervision of Filippo Miatto. She graduated in 2019 with an MSc in Engineering from IMT Atlantique, France. Her current doctoral research focuses on quantum optical neural networks which are variational quantum circuits composed of layers of Gaussian and non-Gaussian transformations.



Filippo Miatto is an Associate Professor at Télécom Paris, he currently works on quantum machine learning and quantum optical circuits. He obtained his PhD in 2012 at the University of Strathclyde (Scotland), followed by two postdoctoral appointments at the University of Ottawa and at the Institute for Quantum Computing (Canada).



Fabio Sciarrino received his PhD degree in physics from the Sapienza University of Rome, Italy, in 2004. He is Full Professor at the Physics Department of the University of Rome La Sapienza and Senior Research Fellow at the International School for Advanced Studies Sapienza, SSAS. He is Principal Investigator of the Quantum Information Lab, Department of Physics, Sapienza University of Rome (www.quantumlab.it). His main expertise is experimental quantum optics, computation and quantum information, and foundations of quantum mechanics. He is currently coordinator of the European FET Open Project PHOQUSING and principal investigator of an ERC (European Research Council) Advanced Grant QU-BOSS.



Ebrahim Karimi was born in Saghez, Kurdistan-Iran. He received the B.Sc. degree in Physics with an emphasis in mathematics from Kerman University in 2001, and M.Sc. from IASBS in 2003, and Ph.D. degree from the University of Naples “Federico II” in 2009. He holds Canada Research Chair in Structured Light at the University of Ottawa. His research focuses on structured quantum waves and their applications in quantum communication, quantum computation, and materials science. He has published over 140 scientific articles in peer-reviewed journals and is co-inventor on three patents. His contributions notably include studies pertaining to the relationship between the quantum spatial properties of photons and their internal properties. Professor Karimi is a Fellow of the OSA, member of the Global Young Academy and The Royal Society of Canada (college of new scholars), Visiting Fellow of the Max Planck Institute for the Science of Light, Fellow of the JCEP, and awarded the Ontario Early Researcher Award in 2018, the University of Ottawa Early Career Researcher of the Year Award in 2019, and the CAP Herzberg Medal in 2020.